

Palaeocene–early Eocene southern subtropical to subpolar silicoflagellate biostratigraphy

KEVIN McCARTNEY¹, JAKUB WITKOWSKI² and ADRIANNA SZARUGA²

¹ Department of Environmental Science and Sustainability, University of Maine at Presque Isle, Presque Isle, ME 04769, USA. E-mail: kevin.mccartney@maine.edu

² Stratigraphy and Earth History Lab, Faculty of Geosciences, University of Szczecin, Mickiewicza 16a, PL-70-383 Szczecin, Poland. E-mails: jakub.witkowski@usz.edu.pl; ada.szaruga@gmail.com

ABSTRACT:

McCartney, K., Witkowski, J. and Szaruga, A. 2018. Palaeocene–early Eocene southern subtropical to subpolar silicoflagellate biostratigraphy. *Acta Geologica Polonica*, **68** (2), 219–248. Warszawa.

Early Palaeocene through early Eocene silicoflagellate assemblages were examined from five southern subtropical through subpolar deep-sea sites: DSDP Holes 208 and 524, and ODP Holes 700B, 752A, and 1121B. For each site, the taxonomic composition of the silicoflagellate assemblage is documented in detail; *Pseudonaviculopsis* gen. nov., *Dictyocha castellum* sp. nov. and *Stephanocha? fulbrightii* sp. nov. are proposed, along with several new combinations. More importantly, however, these observations enable a considerable refinement to the existing Palaeocene–Eocene silicoflagellate biostratigraphic zonation that for the first time uses datums calibrated to the Geomagnetic Polarity Timescale. The *Corbisema aspera* Interval Zone occurs immediately above the K/Pg boundary and is here described from Seymour Island. The *Corbisema hastata* Partial Range Zone extends from near the K/Pg boundary to late early Palaeocene and has been observed in Hole 208. The *Pseudonaviculopsis dissymetrica* Acme Zone occurs in Holes 208 and 700B. The *Dictyocha precarentis* Partial Range Zone, observed in Holes 208, 700B, 752A and 1121B, is subdivided into *D. precarentis*, *Naviculopsis primitiva*, *N. cruciata* and *Pseudonaviculopsis constricta* subzones. The *Naviculopsis constricta* Partial Range Zone occurs in Holes 524, 700B, 752A and 1121B. This study is also the first to consider syn- and/or diachroneity in Palaeogene silicoflagellate biostratigraphy.

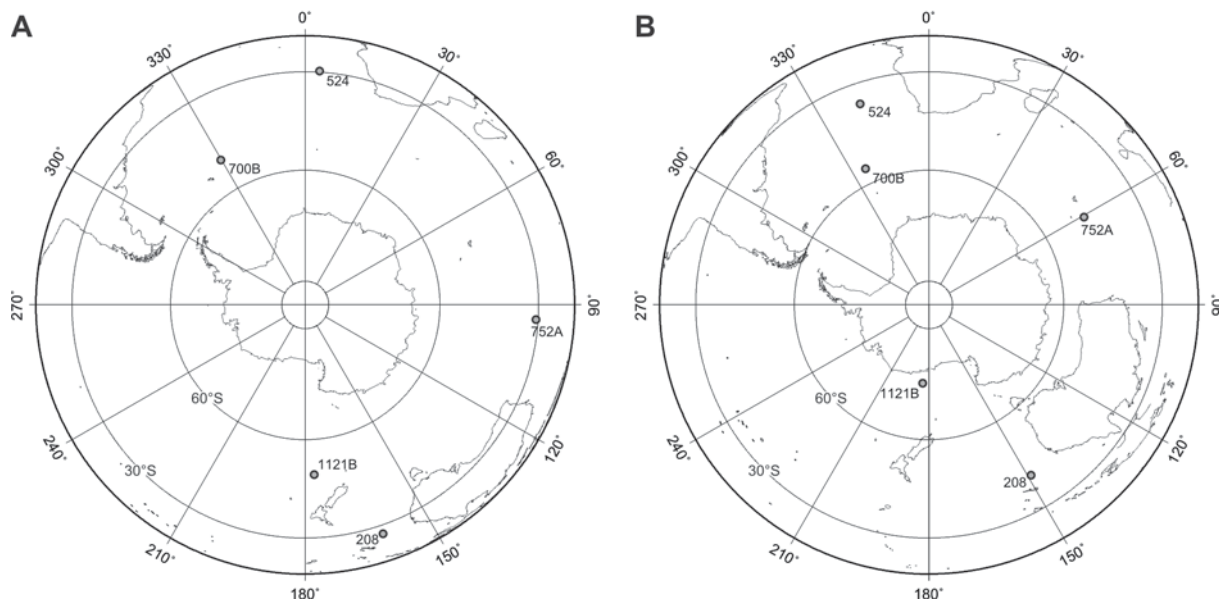
Key words: Palaeocene; Eocene; Biostratigraphy; *Corbisema*; *Dictyocha*; *Naviculopsis*; *Pseudonaviculopsis*.

INTRODUCTION

The verified fossil record of silicoflagellates, marine heterokonts with siliceous skeletons composed of tubular elements, extends from the early Cretaceous to Recent (McCartney *et al.* 2010b), and shows a great morphological diversity in Upper Cretaceous and Palaeogene marine sediments. As part of the plankton, silicoflagellates have a range of important applications in Earth sciences, including biostratigraphy and palaeoceanography (e.g., Whitehead and Bohaty 2003). Their utility, however, is hindered by

two major factors: (1) the sometimes broad limits of skeletal morphological variability that can result in complicated taxonomic interpretation, and (2) opaline silica diagenesis that often limits older silicoflagellate deep sea occurrences to temporally short and geographically widely separated intervals (Barron *et al.* 2015). Yet, our recent work on Cretaceous neritic onshore successions in the Arctic (McCartney *et al.* 2011a, b) clearly shows that in biostratigraphy silicoflagellates sometimes offer a higher resolution than diatom zonal markers.

As in the case of diatoms, early studies of fos-



Text-fig. 1. Maps showing locations for DSDP Holes 208 and 524, and ODP Holes 700B, 752A and 1121B at present (A) and at 58 Ma (B). Base map plotted using Ocean Drilling Stratigraphic Network Advanced Plate Tectonic Reconstruction Service (www.odsnet.de). Palaeolatitude data from Hay *et al.* (1999)

sil silicoflagellates were usually based on material from a limited number of shallow-water sediments exposed on the Eurasian platform (e.g., Schulz 1928; Glezer 1966). Cores retrieved by the Deep Sea Drilling Project, Ocean Drilling Program and Integrated Ocean Drilling Program/International Ocean Discovery Program (DSDP, ODP, IODP, respectively) have greatly enriched silicoflagellate study and at present biostratigraphic zonation are available for the Upper Cretaceous and entire Cenozoic (e.g., McCartney *et al.* 2010b; Bukry 1981, respectively). While Neogene silicoflagellate biostratigraphy is well developed (McCartney *et al.* 1995), early Palaeogene occurrences remain less well studied. This is surprising, as numerous Palaeocene–Eocene siliceous microfossil-bearing successions with reliable age control derived from other microfossil groups have been available for many years.

This study includes microscopic study of silicoflagellates from five deep sea drill cores from southern latitudes (Text-fig. 1A). We have examined this group from Holes 524, 752A and 1121B, all not previously studied for silicoflagellates, and provide the first detailed counts from Hole 208. A portion of Hole 700B was examined here at higher stratigraphic resolution than in the original study by Ciesielski (1991) in order to target an interval that includes the early evolution of the stratigraphically important genus *Naviculopsis*

Frenguelli, 1940. Other significant silicoflagellate evolutionary events considered here include the occurrence of large two-sided silicoflagellates from the middle Palaeocene (*Pseudonaviculopsis* gen. nov.), and an early occurrence of apically-ringed silicoflagellates (*Stephanocha?*) from the early Eocene.

The present study aims to: (1) document the taxonomic composition of hitherto poorly known early Palaeogene deep sea silicoflagellate assemblages, especially in light of recent advances in silicoflagellate taxonomy; (2) present a refined Palaeocene to early Eocene silicoflagellate zonation for southern subtropical to subpolar sites; (3) review the biostratigraphic utility of silicoflagellate datums, and calibrate the age of those datums that appear to have the highest biostratigraphic potential to the Geomagnetic Polarity Timescale (GPTS); and (4) provide an overview of diachroneity in silicoflagellate datums.

MATERIALS AND METHODS

Study sites

In order to provide a temporal framework for the biostratigraphic considerations presented in this study, all silicoflagellate datums (here used interchangeably with ‘bioevents’) are referenced against

the GPTS of Gradstein *et al.* (2012), hereafter referred to as GTS2012. As most of the study sites lack magnetostratigraphy, calcareous nannofossil biostratigraphy is the primary means of age control in this study. The meters below sea level (mbsf) depth of nannofossil zone boundaries are determined through linear interpolation between tie points (Table 1), assuming constant sedimentation rates. Ages were calculated for each sediment sample observed in this study (Tables 2–6). Samples examined in this study come from the following deep sea sites:

DSDP Leg 21, Hole 208 (Table 2)

Site 208 was drilled on the northern Lord Howe Rise, Southwestern Pacific Ocean, northwest of New Zealand. The section recovered at Hole 208 includes a thick interval of middle Eocene to Palaeocene siliceous nannofossil ooze and diatom ooze that was examined for silicoflagellates by Bukry (1973), Dumitrică (1973) and Ling (1981). None of these studies, however, included specimen counts for Site 208. In the present study, we follow the nannofossil and radiolarian biostratigraphy of Hollis (2002). The Palaeocene siliceous microfossil-bearing interval considered in this study spans basal NP3 through basal NP6 calcareous nannofossil zones.

DSDP Leg 73, Hole 524 (Table 3)

Hole 524 was drilled within the Cape Basin, Southeast Atlantic Ocean. Gombos (1984) and Fenner (1991) reported on well-preserved Palaeocene diatoms from a narrow interval within calcareous nannofossil zone NP9 (Percival 1984). Our examination shows that well-preserved silicoflagellates are also present. In this study, we have examined for silicoflagellates the two samples that were reported as diatom-bearing in Gombos (1984).

ODP Leg 114, Hole 700B (Table 4)

Hole 700B was drilled in the East Georgia Basin, South Atlantic Ocean and penetrated a ~90-m thick interval of early Palaeocene through early Eocene nannofossil chalk spanning calcareous nannofossil zones mid-NP4 through upper NP8 (Crux 1991). As no tie points were available from near the bottom of this interval, ages within NP4 are tentatively estimated by interpolating sedimentation rates from the overlying zone NP5. Fenner (1991) and Ciesielski (1991) reported moderately- to well-preserved diatoms and silicoflagellates, respectively, from Hole

	Age (Ma. GTS2012)	Hole 208	Hole 524	Hole 700B	Hole 752A	Hole 1121B
Base NP12	53.70	–		–	115.05	–
Base NP11	54.17	–		–	143.97	–
Base NP10	55.86	–		242.95	171.10	–
Base NP9	57.21	–	33.45	247.65	202.82	–
Base NP8	58.70	–	62.15	273.12	219.50	50.60
Base NP7	58.97	–			225.77	77.00
Base NP6	59.54	543.50		274.15	252.60	110.00
Base NP5	61.61	550.50		293.82		134.40
Base NP4	63.25	561.50		–		–
Base NP3	64.81	576.00		–		–

Table 1. Mbsf depths for the base of nannofossil zones, using ages from Gradstein *et al.* (2012)

700B. Our study concentrates to obtain a more detailed record of the interval that includes *Naviculopsis primitiva* Ciesielski, 1991 and *N. cruciata* Ciesielski, 1991. Other biozone boundaries are interpreted from Ciesielski's (1991) range charts.

ODP Leg 121, Hole 752A (Table 5)

Hole 752A was drilled on Broken Ridge in the Eastern Indian Ocean and recovered a ~200 m-thick middle Palaeocene–early Eocene siliceous microfossil-bearing interval spanning calcareous nannofossil zones NP2 through NP12. Diatoms are the only siliceous microfossil group studied to date from Hole 752A (Fourtanier 1991). Following Barron *et al.* (2015), who have calibrated some of the diatom datums established by Fourtanier (1991) to GTS2012, we use the nannoplankton data from Pospichal *et al.* (1991) as tie points for the age model used in this study.

ODP Leg 181, Hole 1121B (Table 6)

Hole 1121B was drilled on the Campbell Plateau margin in the Southwestern Pacific Ocean, and penetrated a ~100 m-thick siliceous microfossil bearing interval of Palaeocene age. Although abundant and well-preserved diatoms were observed within the upper ~60 m of this unit (Fenner 2015), silicoflagellates have not been studied from Hole 1121B to date. Hollis (2002) reported on diverse radiolarian assemblages from this hole and showed siliceous fossils to occur over an interval spanning mid-NP5 through basal NP8 calcareous nannofossil zones.

Sample and slide preparation and observation

Prior to processing, samples were placed in 60 ml plastic containers and freeze-dried for 24 hours.

DSDP Sample number	SZCZ Sample number	Depth (mbsf)	Age (Ma, GTS2012)	Stage	Nannofossil Zone	Silicoflagellate Zone	Silicoflagellate Subzone	Number of slides counted	<i>Corbisema apiculata</i>	<i>C. archangeliskiana</i>	<i>C. archangeliskiana</i> (basal spines)	<i>C. archangeliskiana</i> (four-sided)	<i>C. camara</i>	<i>C. cunicula</i>	<i>C. falklandensis</i>	<i>C. hastata s. ampl.</i>	<i>C. hastata alta</i>	<i>C. hastata globulata</i>	<i>C. hastata minor</i>	<i>C. inermis</i>	<i>C. inermis</i> (with spines)	<i>C. inermis crenulata</i>	<i>C. inermis minor</i>	<i>C. triacantha s. ampl.</i>	<i>C. cf. trigona</i>	<i>Dicryochoa precarentis</i> (five-sided)	<i>N. primitiva</i>	<i>Pseudonaviculopsis dissymmetrica</i>	<i>P. constricta</i>	<i>P. naviculoides</i>	Total silicoflagellates			
21-208-29R-2, 105-106	24299	541.55	58.54	Late Pal.	NP6	un zoned	1																								0			
21-208-29R-3, 25-26	24300	542.25	58.90				1																										0	
21-208-29R-3, 105-106	24301	543.05	59.31				1																										0	
21-208-29R-4, 25-26	24302	543.75	59.61	Middle Palaeocene	NP5	<i>Dicryochoa precarentis</i> Zone	<i>N. pr.</i>	3	5	2			2	2		8	4	1		5				4	3	1	2	1	4	1	2	47		
21-208-29R-4, 105-106	24303	544.55	59.84					2	3	5			3			2			2			5				1	2		8			1	6	36
21-208-29R-5, 25-26	24304	545.25	60.03					1	7	1			2			1	7					4					1		13			10	46	
21-208-29R-5, 105-106	24305	546.05	60.26					1	2							1						1				1			4			2	11	
21-208-29R-6, 25-26	24306	546.75	60.45					1	3							2																4	9	
21-208-29R-6, 105-106	24307	547.55	60.68					1	4	1			1			2			2	1	3										4	8	24	
21-208-30R-1, 50-51	22853	548.50	60.95					2	4	6	5	13				18			5	1	2					15	23	19	11		42	29	5	198
21-208-30R-1, 100-101	22854	549.00	61.09					2	2	2	2	3	3			6	2									5	9		5		14	15		66
21-208-30R-2, 50-51	22855	550.00	61.37					2	3	5	3	8	3			5	1				4					4	14	3	3		49	45		150
21-208-30R-2, 99-100	22856	550.50	61.51					2	4			4				5	2				4	1(sp)				3	2				24	17		65
21-208-30R-3, 50-51	22857	551.50	61.67					1	3							14	4										7	4						32
21-208-30R-3, 100-101	22858	552.00	61.75					1																			1				65	16		82
21-208-30R-4, 50-51	22859	553.00	61.91					1	2			3				25	4	7	2	1	1	1	1	1	1	2	3			83	25		159	
21-208-30R-5, 101-102	22861	555.00	62.22					1	4			5				14	6	5	15	21								2						72
21-208-30R-6, 50-51	22862	556.00	62.38					1	2			5				12	2	2	5	4	1						15	2				1		51
21-208-30R-CC	22864	557.00	62.54					1	6	2	1	4	1			29	13	8	11							1								76
21-208-31R-1, 125-126	24066	559.25	62.89					1	3	1						8	5	7	4															28
21-208-31R-2, 50-51	22865	560.00	63.01					1				1				4							1									1		7
21-208-31R-2, 145-146	24068	560.95	63.16	1	1			1				14	4	4										1						25				
21-208-31R-3, 50-51	22866	561.50	63.25	1	7	1		4				18	6	4	1								4					1		46				
21-208-31R-3, 145-146	24070	562.45	63.37	1	1				1			11	1	2	2									1						19				
21-208-31R-4, 85-86	24071	563.35	63.47	1	2							19	3		2	2	1(sp)						3							31				
21-208-31R-4, 145-146	24073	563.95	63.55	1	1	1						6	1	1	1	2	1													14				
21-208-31R-5, 45-46	24075	564.45	63.61	1		1						5	3	5		3	1						2							20				
21-208-31R-6, 95-96	24076	566.45	63.85	1					1			3	2	3																9				
21-208-31R-6, 145-146	24077	566.95	63.91	1								9	5	7									2							23				
21-208-31R-CC	22867	567.00	63.92	1	1																	1					6	1		9				

Table 2. Silicoflagellate specimen counts from DSDP Hole 208; (sp) refers to specimens that have corner spines

Between 1.5 and 2.0 g of dried sample was then placed in a 50-ml Nunc® centrifuge tube and treated with 10% HCl in order to dissolve carbonate. Organic matter was oxidized for at least three hours at 100°C

in a shaking water bath using 37% H₂O₂. Samples were then decanted and washed multiple times in de-ionized water. Random settling method was applied to prepare microscope slides. Four 18 × 18 mm cover-

DSDP Sample number	SZCZ Collection number	Depth (mbsf)	Age (Ma, GTS2012)	Stage	Nannofossil Zone	Silicoflagellate Zone	Number of slides counted	<i>Corbisema archangelskiana</i>	<i>C. bimucronata elegans</i>	<i>C. camera</i>	<i>C. cunicula</i>	<i>C. hastata s. ampl.</i>	<i>C. hastata globulata</i>	<i>C. hastata minor</i>	<i>C. inermis inermis</i>	<i>C. triacantha s. ampl.</i>	<i>Naviculopsis cf. americana</i>	<i>N. constricta</i>	<i>N. danica</i>	<i>N. eobiapiculata</i>	<i>Pseudonaviculopsis constricta</i>	Total silicoflagellates
524-4R-3, 87–89	1119	51.38	56.50	late	NP9	<i>N.</i>	1	1	2		9	2	6			1	2	13	8	4		48
524-5R-1, 69–71	1120	57.50	56.89	Palaeocene		<i>constr.</i>	2	6	2		1	8	2	5	3	3		7	3	5	1	46

Table 3. Silicoflagellate specimen counts from DSDP Hole 524

ODP Sample number	SZCZ Collection number	Depth (mbsf)	Age (Ma, GTS2012)	Stage	Nannofossil Zone	Silicoflagellate Subzone	Number of slides counted	<i>Corbisema apiculata</i>	<i>C. archangelskiana</i>	<i>C. archangelskiana</i> (four-sided)	<i>C. camera</i>	<i>C. cunicula</i>	<i>C. falklandensis</i>	<i>Corbisema hastata s. ampl.</i>	<i>C. hastata globulata</i>	<i>C. hastata minor</i>	<i>C. hastata alta</i>	<i>C. inermis inermis</i>	<i>C. inermis crenulata</i>	<i>C. inermis minor</i>	<i>C. triacantha s. ampl.</i>	<i>Dityocha precarentis</i> five-sided	<i>Naviculopsis constricta</i>	<i>N. cruciata</i>	<i>N. primitiva</i>	<i>Pseudonaviculopsis dissymetrica</i>	<i>P. constricta</i>	Total silicoflagellates	
114-700B-30R-1, 79–80	24043	276.80	59.67	Middle Palaeocene	NP5	<i>Ps. constricta</i>	1	24	24		13	158	14	10	5			11	1	3	17	37	1	1?		6	21	345	
114-700B-30R-1, 99–101		277.00	59.69						see Ciesielski (1991) for data																				
114-700B-30R-1, 121–122	23848	277.20	59.71					<i>N. cruciata</i>	1	19	33	23	301	1	13	8	2	1	43	1	5	14	32	3	80		40	68	687
114-700B-30R-1, 135–136	24046	277.35	59.73					<i>N. cruciata</i>	1	14	4	4	64	1					10		2	2	2		74		1	3	181
114-700B-30R-1, 145–146	24047	277.45	59.74					<i>N. primitiva</i>	1	33	25	1	16	244	1	18	4	1	19	5	15	4	2	1	3	266		1	659
114-700B-30R-2, 25–26	23849	277.75	59.77					<i>N. primitiva</i>	1	8	9	10	14	1	1	2	2		2		1	2	1	1			77		131
114-700B-30R-2, 69–70	23850	278.20	59.82					<i>N. primitiva</i>	1	3	1	3	3		4	1	3	1	2				1			32			54
114-700B-30R-2, 118–120		278.69	59.87						see Ciesielski (1991) for data																				
114-700B-30R-2, 120–121	23851	278.70	59.87					<i>N. primitiva</i>	1	15	6	10	2	3	7	2	2	12	3	9							66		137
114-700B-30R-3, 5–6	24050	279.05	59.91					<i>N. primitiva</i>	1	22	7	15	7		27	5	2	5	54	27	5	4					94		274
114-700B-30R-3, 26–27	24378	279.26	59.93					<i>N. primitiva</i>	1	13	11	5	5		6	1	1	32	28	6	3	2				34			147
114-700B-30R-3, 43–44	23479	279.43	59.95					<i>D. precarentis</i>	1	38	9	12	23	3	13	4	3	311	34	4	7	9							470
114-700B-30R-3, 105–106	24051	280.05	60.02					<i>D. precarentis</i>	1	18	9	1	4	27	3	28	1	159	42	13	8	14	9						336
114-700B-30R-3, 106–108		280.07	60.02						see Ciesielski (1991) for data																				

Table 4. Silicoflagellate specimen counts from the *Naviculopsis primitiva* and *N. cruciata* subzones in Hole 700B. Intervals for which additional data is available in Ciesielski (1991) are also shown

slips were set into a Petri dish that was subsequently filled with deionized water. Depending on sample density, between 1.0 and 3.0 ml of the chemically treated residue was pipetted into the Petri dish which was left to evaporate naturally. Coverslips were mounted on slides using Naphrax diatom mountant (refractive index = 1.73).

Light microscope (LM) examination was performed with a Nikon Eclipse E600 microscope, with specimen counts made using ×200 magnification. The entire microscope slide was examined with all

identifiable fragments representing more than half the original specimen counted. Additional slides were counted when rare or interesting taxa were sought; the number of slides examined for each sample is listed in Tables 2–6. Photographs for this publication were made with a Leica DMLB microscope using a ×50 oil immersion objective and Nikon DS-Fi1 camera. To avoid presenting multiple focal depths for each of the specimens depicted on plates, light micrographs were spliced using the freeware software Picolay (available online at www.picolay.de).

ODP Sample number	SZCZ Collection number	Depth (mbsf)	Age (Ma, GTS2012)	Stage	Nannofossil Zone	Silicoflagellate Zone	Silicoflagellate Subzone	Number of slides counted	<i>Corbisema apiculata</i>	<i>C. archangeliskiana</i>	<i>C. archangeliskiana</i> (four-sided)	<i>C. aff. apiculata</i>	<i>C. bimucronata elegans</i>	<i>C. camera</i>	<i>C. cunicula</i>	<i>C. falklandensis</i>	<i>Corbisema hastata s. ampl.</i>	<i>C. hastata globulata</i>	<i>C. hastata minor</i>	<i>C. hastata alia</i>	<i>C. inermis inermis</i>				
																						NP11	NP10	NP9	NP8
752A-14X-1, 50-51	24257	123.10	53.83	Early Eocene	NP11	Silicoflagellate Zone		2									1	1							
752A-14X-2, 50-51	24258	124.60	53.86					2													2				
752A-14X-3, 63-65	18014	126.23	53.88					3	4									1			4	3			4
752A-14X-3, 120-121	24259	127.20	53.90					2							3						2				
752A-14X-4, 49-50	24260	128.0	53.91					3	6						8				1		3				1
752A-14X-5, 20-21	24261	129.20	53.93					3	6						1										1
752A-15X-1, 121-122	23983	133.51	54.00					2	1										2		1				
752A-15X-2, 50-51	24263	134.30	54.01					1																	
752A-15X-3, 50-51	23264	135.80	54.04					2													4				
752A-15X-4, 62-64	18015	137.42	54.06					2	1									1			3				1
752A-15X-5, 49-50	24266	138.80	54.09					2	3									1			2				
752A-16X-1, 50-51	24267	142.50	54.15					1	6						2			4	4	1	4	14	2		1
752A-16X-2, 120-121	23984	144.70	54.22					1													1				
752A-16X-5, 25-27	18016	148.25	54.44					1													1				
752A-17X-2, 120-122	18017	154.40	54.81					2										1	1		3				1
752A-18X-2, 10-12	18018	163.00	55.36					1													2	10			f
752A-19X-1, 120-122	18019	172.30	55.91					1																	f
752A-19X-2, 62-64	18020	173.8	55.97					2	2	6															1
752A-19X-3, 53-55	18021	174.63	56.01					2	2	7								1			4				
752A-19X-4, 99-101	18022	176.24	56.08	2	4	3											1	1			3				
752A-20X-1, 81-82	23988	181.50	56.30	1									1	4			5				2				
752A-20X-cc	23991	182.99	56.37	1	3							1	1	28			7		1		4				
752A-21X-2, 100-102	18024	192.91	56.79	1								1	1?				9								
752A-22X-2, 119-120	18025	202.79	57.21	1		f																			
752A-22X-4, 16-17	23993	204.76	57.27	1	2						1		15			5		1			4				
752A-23X-1, 118-120	18026	210.98	57.45	2	3	10					2		5		33				5		15				
752A-23X-CC, 10-11	23994	211.66	57.53	1	2								15			3									
752A-24X-1, 99-101	23995	220.49	58.74	1	2	2					1	1				2		5			6				
752A-24X-2, 97-99	18027	221.97	58.81	2	3	7	1				4		7		37						10				
752A-25X-1, 122-123	23996	230.32	59.07	1	10	4						7	3		18	6		2			11				
752A-25X-2, 54-56	18028	231.14	59.09	2	13	19					1	2			28				3		8				
752A-26X-2, 124-125	23997	241.54	59.32	1	1	1						3	6		6	1		2							
752A-26X-5, 120-121	23998	246.00	59.42	1	2	2						4			5	2	1								
752A-27X-1, 129-130	23999	249.69	59.50	2	1	3						16	6		14	9	9	7			14				
752A-27X-3, 128-130	24000	252.68	59.60	1	6	1						8	4		5	4	2				1				
752A-27X-4, 50-51	24072	253.40	59.64	1	2	1						12	21		4		1				9				
752A-27X-4, 80-81	24073	253.70	59.66	1	11	8						16	27		18	2	1				8				
752A-28X-1, 16-17	24074	258.26	59.91	1	6	4						2	12	1	22	1	1				14				
752A-28X-2, 36-37	24283	258.46	59.92	1	20	17						32	44		16	3	23	4			57				
752A-28X-2, 116-117	24001	260.76	60.05	2	19	4						62	7	1	15	7	3				28				
752A-28X-2, 126-127	24289	260.86	60.05	1	5	4						13			4						12				
752A-28X-3, 20-21	24291	261.3	60.08	1	6	4						8	1		3				5		34				
752A-28X-3, 95-96	24384	262.05	60.12	1	2	2						2	1		2	1	1				8				
752A-28X-4, 20-21	24293	262.8	60.16	1	3	4						1	1		6						11				
752A-28X-4, 60-61	24386	263.2	60.18	1	4	2						2			4	1					4				
752A-28X-4, 120-121	24295	263.8	60.22	2	1	4						5	5		9	2		17			9				
752A-28X-5, 117-118	24002	265.27	60.30	2	10	2						3	1		18	1	4	3							
752A-29X-3, 61-63	18029	270.71	60.60	2	3	14						1			7						4				

Table 5. Silicoflagellate specimen counts from ODP Hole 752A

ODP Sample number	<i>C. inermis crenulata</i>	<i>C. inermis minor</i>	<i>C. triacantha</i> s. ampl.	<i>Dictyochoa</i> cf. <i>byronalis</i>	<i>D. precarenis</i>	<i>D. precarenis</i> s. ampl. five-sided	<i>D. castellum</i> n. sp.	<i>Naviculopsis</i> cf. <i>americana</i>	<i>N. constricta</i>	<i>N. cruciata</i>	<i>N. eobiapiculata</i>	<i>N. eobiapiculata</i> , apex spine	<i>N. foliacea</i>	<i>N. minor</i>	<i>N. cruciata</i>	<i>N. primitiva</i>	<i>Pseudonaviculopsis dissymmetrica</i>	<i>P. constricta</i>	<i>P. cuspis</i>	<i>P. naviculoidea</i>	<i>Stephanocha?</i> aff. <i>acanthicus</i>	<i>Stephanocha?</i> aff. <i>fulbrightii</i> sp. nov.	Total silicoflagellates
752A-14X-1, 50-51			8	1		5			20		5			3				1			1		46
752A-14X-2, 50-51		1	2			2			12		1			1				1			1		23
752A-14X-3, 63-65			15	2		8			19					13								1	74
752A-14X-3, 120-121			5	1		3			19		1		1?	4				2					40
752A-14X-4, 49-50		1	3			25	2		28		5			4				2					89
752A-14X-5, 20-21	2		5			19	2	3	41		3		3?	4								3	90
752A-15X-1, 121-122			2	1		1	1	2	2					2									15
752A-15X-2, 50-51						1																	1
752A-15X-3, 50-51			2					9	3									1				1	20
752A-15X-4, 62-64			6	2		2		24	4					1					2			1	48
752A-15X-5, 49-50						11	1	25	4														47
752A-16X-1, 50-51			1			25		83	39		1							2				1	190
752A-16X-2, 120-121			1			1		4	1														8
752A-16X-5, 25-27													1?										1
752A-17X-2, 120-122			1	2				2	3										1				15
752A-18X-2, 10-12									9		1												22
752A-19X-1, 120-122																							0
752A-19X-2, 62-64			4						14		3	1		5									36
752A-19X-3, 53-55			20						22					12				5					73
752A-19X-4, 99-101			3						29		28	2						5	2				81
752A-20X-1, 81-82			2						8		20	12		3									57
752A-20X-cc			21						41		3			1									111
752A-21X-2, 100-102									7											1			18
752A-22X-2, 119-120																							0
752A-22X-4, 16-17			7						6									4					45
752A-23X-1, 118-120		1	8						15									15					112
752A-23X-CC, 10-11			2		4				9									6					41
752A-24X-1, 99-101		1	7		26		1		1									7					62
752A-24X-2, 97-99			26		89				1									2	1	2			190
752A-25X-1, 122-123		2	8		83		1		1									4					160
752A-25X-2, 54-56			19		54				4									1					152
752A-26X-2, 124-125		1	7		4													2					34
752A-26X-5, 120-121	1?		1		1												2						20
752A-27X-1, 129-130			4		23		6											2		1			115
752A-27X-3, 128-130			4		2		1											8					46
752A-27X-4, 50-51			8		1		1								3			4	11				78
752A-27X-4, 80-81			7		10		3								23			9	7				150
752A-28X-1, 16-17		1	20																	51			135
752A-28X-2, 36-37		5	25		1		1													126			374
752A-28X-2, 116-117		4	11																	83			244
752A-28X-2, 126-127			5																	38			81
752A-28X-3, 20-21		1	8				1													35			106
752A-28X-3, 95-96		1	8		1															28			57
752A-28X-4, 20-21			3																	20			49
752A-28X-4, 60-61																				4			21
752A-28X-4, 120-121		1	7				1									1?	1						62
752A-28X-5, 117-118			7		1																		50
752A-29X-3, 61-63		1	2		6																		40

Table 5 – continued

ODP Sample number	SZCZ Collection number	Depth (mbsf)	Age (Ma, GTS2012)	Stage	Nannofossil Zone	Silicoflagellate Zone														
						Number of slides counted	<i>Corbisema apiculata</i>	<i>C. archangeliskiana</i>	<i>C. canara</i>	<i>C. cunicula</i>	<i>C. falklandensis</i>	<i>C. hastata s. ampl.</i>	<i>C. hastata globulata</i>	<i>C. hastata minor</i>	<i>C. inermis inermis</i>	<i>C. inermis minor</i>	<i>C. inermis crenulata</i>	<i>C. triacantha s. ampl.</i>		
181-1121B-6X-1, 85–86	23896	33.55	57.29	Late Palaeocene	NP8	<i>N. con.</i>	2		5	9	2		18	5	2	6	4		6	
181-1121B-6X-2, 70–71	24125	34.90	57.4			2	5	6	9	1	4	13	5	1	7					9
181-1121B-7X-1, 100–101	23897	43.30	58.1			2	2	3	4	4	3	4	4		5	3	1	4		
181-1121B-7X-3, 116–117	23898	46.46	58.36			2		2	4	5	2	4	1	6	10	1	1	4		
181-1121B-7X-5, 120–121	24126	49.50	58.61			2	3	5	14	6	2	10	5	2	6	2				15
181-1121B-8X-1, 86–87	23899	52.86	58.77		1	3	3	4	22	1	5	3	6	2	3				6	
181-1121B-8X-3, 116–117	23900	56.16	58.88		1		3	2	16		4	1		1	2				5	
181-1121B-8X-5, 94–95	23901	58.94	58.97		1	1	4	11		1	3	2	4	6					5	
181-1121B-9X-1, 66–67	23902	62.26	59.07		1	2	1	2				1		6					2	
181-1121B-9X-3, 91–93	23903	65.51	59.17		1	3	1	13	3		3	8	1	9	1				2	
181-1121B-9X-5, 83–84	23904	68.43	59.27		1	7	8	24	1		18	12	4	3	1	1				
181-1121B-10X-1, 107–108	24905	72.27	59.39		1	6	4	3	1	1	7	2	2						1	
181-1121B-10X-2, 110–111	24127	73.80	59.44		1	1	4	5	2	1	3		11	14		4	5			
181-1121B-10X-3, 115–116	23906	75.35	59.49		1	1	6	6	2	1	2	2	1						5	
181-1121B-10X-4, 50–51	24128	76.80	59.53		1	3	3	7			1		4	10					2	
181-1121B-10X-1, 20–21	24470	81.10	59.78	1	6	10	17	4	1	20	10	3	35	4				26		
181-1121B-11X-1, 135–136	23907	82.25	59.85	1	2	31	10	4	3	16	4	9	4	1	1	11				
181-1121B-11X-2, 140–141	24134	83.80	59.95	1	15	19	25	7	4	34	2	9	32					19		
181-1121B-11X-3, 83–84	23908	84.73	60.00	1	3	35	7	3	1	18	1	31	7	1				18		
181-1121B-11X-4, 94–95	23909	86.34	60.10	1	5	8	3		1	5	7	5	5					3		
181-1121B-12X-1, 100–101	24144	91.50	60.41	1	4	4	16	1	3	20	11	6	26		1	8				
181-1121B-12X-2, 100–101	24145	93.00	60.50	1	21	15	22	3	5	29	9	8	37	14		37				
181-1121B-12X-3, 40–41	24146	93.90	60.55	1																
181-1121B-13X-1, 10–11	24147	100.20	60.92	0.5																
181-1121B-14X-1, 10–11	24148	109.80	61.50	0.5																
181-1121B-15X-1, 100–101	24149	120.40	62.04	NP4	0.5															

Table 6. Silicoflagellate specimen counts from ODP Hole 1121B

	Hole 208, palaeolatitude 43°S			Hole 752A, palaeolatitude 49°S		
	Depth (mbsf)	Correlation	Age (Ma, GTS2012)	Depth (mbsf)	Correlation	Age (Ma, GTS2012)
FCO <i>N. constricta</i>	–	–	–	236.34±5.2	mid-NP6	59.21
LO <i>N. cruciata</i>	–	–	–	253.04±0.36	uppermost NP5	59.62
LO <i>N. primitiva</i>	–	–	–	255.98±2.28	uppermost NP5	59.78
FCO <i>N. primitiva</i>	544.15±0.4	uppermost NP5	59.72	263.5±0.3	upper NP5	60.2
FO <i>D. precarentis</i>	550.25±0.25	basal NP5	61.44	–	–	–
FO <i>Ps. disymmetrica acme</i>	554.0±1.0	upper NP4	62.06	–	–	–
FO <i>C. hastata</i>	567.0	NP3	63.92	–	–	–

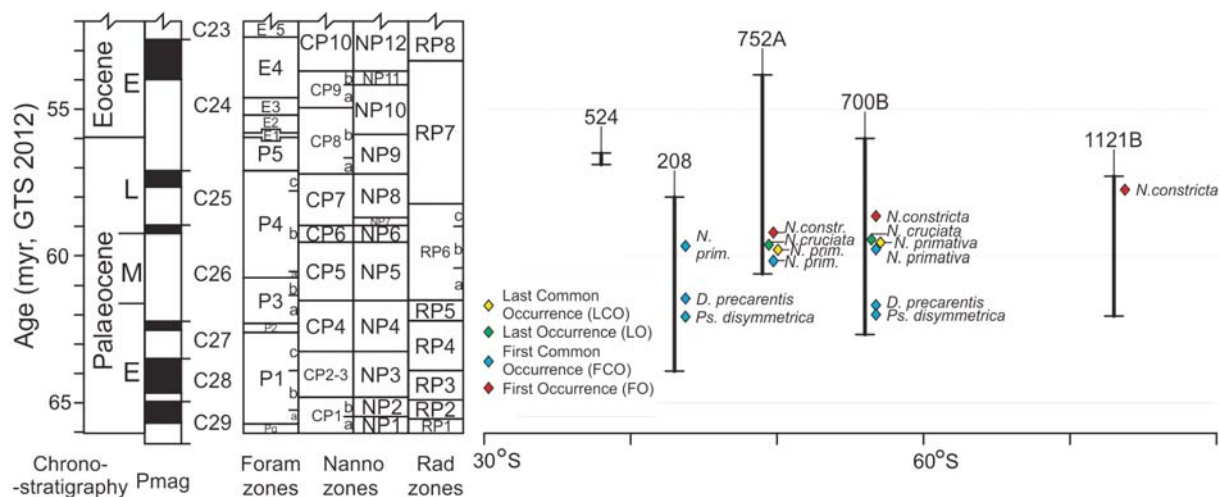
Table 7. Age calibration of silicoflagellate datums for Holes 208, 700B, 752A and 1121B

ODP Sample number	SZCZ Collection number	Depth (mbsf)	Age (Ma, GTS2012)	Stage	Nannofossil Zone	Silicoflagellate Zone										Total silicoflagellates	
						<i>Dicryochoa precarentis</i> with apical plate	five-sided	<i>Naviculopsis constricta</i>	<i>N. primitiva</i>	<i>Pseudonaviculopsis dissymmetrica</i>	<i>P. constricta constricta</i>	<i>P. constricta spinosa</i>	<i>P. naviculoides</i> with corner spines	<i>P. cuspis</i>			
181-1121B-6X-1, 85–86	23896	33.55	57.29	Late Palaeocene	NP8	<i>N. con.</i>	39		1	3	20	1	2			97	
181-1121B-6X-2, 70–71	24125	34.90	57.4				80		1	5	1	26		2		2	146
181-1121B-7X-1, 100–101	23897	43.30	58.1				34	1			22	19		1	1	1	72
181-1121B-7X-3, 116–117	23898	46.46	58.36		27	1			31	43		5		2	68		
181-1121B-7X-5, 120–121	24126	49.50	58.61		41				23	27		3			111		
181-1121B-8X-1, 86–87	23899	52.86	58.77		27				8	59		2			85		
181-1121B-8X-3, 116–117	23900	56.16	58.88		24				1	9	1				58		
181-1121B-8X-5, 94–95	23901	58.94	58.97		39	2	1		5	16	1	2	3		79		
181-1121B-9X-1, 66–67	23902	62.26	59.07		16	1			8	15		1	5		31		
181-1121B-9X-3, 91–93	23903	65.51	59.17		44	2			37	189	5	4	11	2	90		
181-1121B-9X-5, 83–84	23904	68.43	59.27		119	10			7	161	2	2	19	2	208		
181-1121B-10X-1, 107–108	24905	72.27	59.39		49	5	1			5	7				82		
181-1121B-10X-2, 110–111	24127	73.80	59.44		34				5	5		1	6	1	84		
181-1121B-10X-3, 115–116	23906	75.35	59.49		38				1	10	3				64		
181-1121B-10X-4, 50–51	24128	76.80	59.53		20				1	1		1	1		50		
181-1121B-10X-1, 20–21	24470	81.10	59.78	126				6	34				4	262			
181-1121B-11X-1, 135–136	23907	82.25	59.85	78		1		11	25		6			175			
181-1121B-11X-2, 140–141	24134	83.80	59.95	223		1		3	23		5		1	390			
181-1121B-11X-3, 83–84	23908	84.73	60.00	196				7	36		6		3	321			
181-1121B-11X-4, 94–95	23909	86.34	60.10	17				3	12		2			59			
181-1121B-12X-1, 100–101	24144	91.50	60.41	73			1	134	96		7	1	2	414			
181-1121B-12X-2, 100–101	24145	93.00	60.50	160		1		8	54	1	3	4		361			
181-1121B-12X-3, 40–41	24146	93.90	60.55						1					1			
181-1121B-13X-1, 10–11	24147	100.20	60.92											0			
181-1121B-14X-1, 10–11	24148	109.80	61.50											0			
181-1121B-15X-1, 100–101	24149	120.40	62.04		NP4									0			

Table 6. – continued

	Hole 700B, palaeolatitude 56°S			Hole 1121B, palaeolatitude 73°S		
	Depth (mbsf)	Correlation	Age (Ma, GTS2012)	Depth (mbsf)	Correlation	Age (Ma, GTS2012)
FCO <i>N. constricta</i>	272.185±3.815	basal NP8	58.68	39.1±4.2	upper NP8	57.75
LO <i>N. cruciata</i>	276.9±0.1	uppermost NP5	59.68	–	–	–
LO <i>N. primitiva</i>	277.4±0.05	uppermost NP5	59.74	–	–	–
FCO <i>N. primitiva</i>	279.345±0.085	uppermost NP5	59.94	–	–	–
FO <i>D. precarentis</i>	295.15±0.25	uppermost NP4	61.66	–	–	–
FO <i>Ps. dissymmetrica</i> acme	297.625±0.775	upper NP4	61.96	–	–	–
FO <i>C. hastata</i>	301.4	NP4	62.67	–	–	–

Table 7 – continued



Text-fig. 2. Age calibration of silicoflagellate datums from Holes 208, 524, 700B, 752A and 1121B, plotted versus palaeolatitude

Scanning electron microscopy (SEM) was performed at Warsaw University of Technology using a Hitachi S8000 instrument, and at West Pomeranian University of Technology in Szczecin, using Hitachi SU8020. Raw and processed material and slides are curated in the Institute of Marine Sciences, University of Szczecin Diatom Collection (SZCZ); herbarium numbers for all samples and slides are included in Tables 2–6.

RESULTS

This study documents the occurrence of 33 silicoflagellate taxa, most of which are included in the three genera (*Corbisema* Hanna, 1928, *Dictyocha* Ehrenberg, 1839 and *Naviculopsis* Frenguelli, 1940) well known from the early Palaeogene. In addition, a group of naviculopsid morphologies that predate the evolution of *Naviculopsis* are here placed into a new genus *Pseudonaviculopsis*. The early Eocene of Hole 752A includes several unusual silicoflagellate occurrences that include a new species of *Dictyocha* and another that is tentatively placed in *Stephanocha*.

Silicoflagellate datums

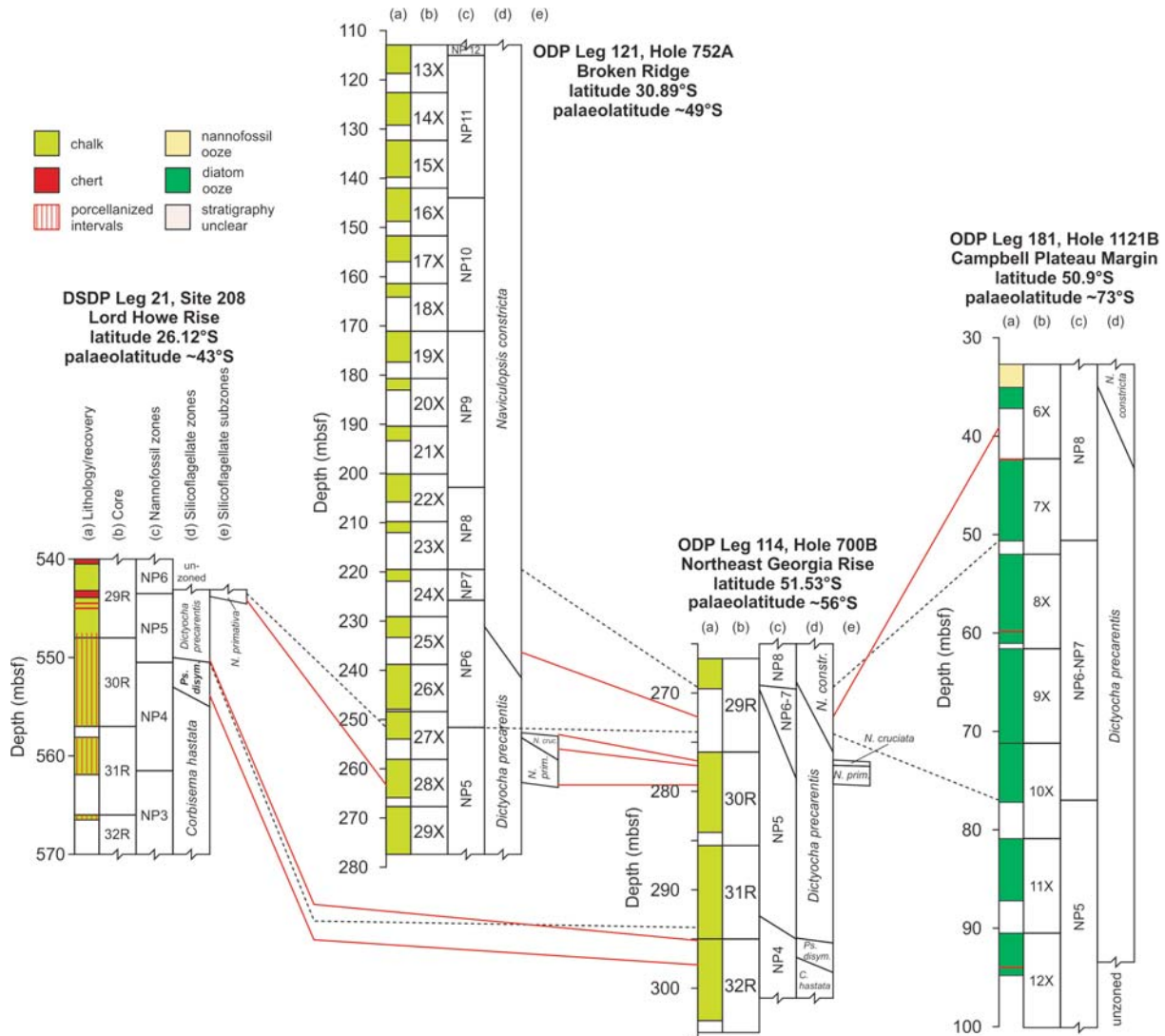
Samples that mark the highest and lowest observed occurrences of biostratigraphically useful taxa are provided in this section as mbsf depths, with citation to the relevant table. Bioevents are identified as first occurrence (FO), last occurrence (LO),

first common occurrence (FCO) or last common occurrence (LCO) of taxa and plotted against age and palaeolatitude (Text-fig. 2). These bioevents are proposed as zonal and subzonal markers in this study.

FCO *Pseudonaviculopsis disymmetrica* is used here as a primary zonal marker, with abundant *Ps. constricta* as a secondary zonal marker. Both species have an abundance acme in Holes 208 and 700B. The observed lower limit of this interval is at 553.0 mbsf in Hole 208 (Table 2) and at 296.85 mbsf in Hole 700B (Ciesielski 1991).

FO *Dictyocha prearentis* is used as a zonal marker and shows the first common appearance of four-sided silicoflagellate skeletons (*Dictyocha*) in the Cenozoic. This marker was observed in Hole 208 at 550.0 mbsf (Table 2) and at 294.9 mbsf in Hole 700B (Ciesielski 1991). *Naviculopsis primitiva* and *N. cruciata* are used as subzonal markers. In Hole 752A, FCO and LO *Naviculopsis primitiva* are observed at 263.2 and 258.26 mbsf, respectively, and LO *N. cruciata* at 253.4 mbsf (Table 5). These two taxa were described by Ciesielski (1991) from Site 700B, and we have reexamined that sequence to find FCO and LO *N. primitiva* at 279.26 and 277.45 mbsf, respectively (Table 4), and LO *N. cruciata* at 277.0 mbsf (Ciesielski 1991). FCO *N. primitiva* was also observed at 543.75 mbsf in Hole 208 (Table 2).

Naviculopsis constricta has observed FCOs in Holes 752A (231.14 mbsf) and 1121B (34.9 mbsf). Ciesielski (1991) records FCO *N. constricta* at 268.37 mbsf in Hole 700B. The next higher zonal marker, FCO *N. foliacea* (Bukry and Foster 1974), was not observed in this study.



Text-fig. 3. Fence diagram showing nannofossil- and silicoflagellate-based correlation of Holes 208, 752A, 1121B and 700B. Stratigraphic columns are arranged according to increasing palaeolatitude

Biostratigraphy

The following biostratigraphic zonation (Text-fig. 3) for the Palaeocene–lower Eocene southern subtropical to subpolar sites is proposed. Bioevent boundaries are interpreted as the midpoint between observed occurrences, with those depths and ages shown in Table 7 and identified by “~” below.

Corbisema aspera Interval Zone

DEFINITION: Interval (gap) between the LO *Lyrulima furcula* and the FO *Corbisema hastata*.

AUTHORS: Harwood, McCartney, Witkowski and Szaruga (this report).

REMARKS: This zone is based on observations by Harwood (1988) from immediately above the K/Pg boundary and is not observed in this study.

ASSEMBLAGE: Harwood (1988) observed small numbers of several taxa, the most abundant being *C. aspera*.

OCCURRENCE: The zone is only known from southern Seymour Island.

***Corbisema hastata* Partial Range Zone**

DEFINITION: Interval from the FO *Corbisema hastata* up to the base of the *Pseudonaviculopsis dissymmetrica* Acme Zone.

AUTHORS: Bukry and Foster (1974); top emended in this paper.

ASSEMBLAGE: Silicoflagellates in this interval are almost exclusively *Corbisema* spp. with *C. hastata*, *C. archangelskiana* and *C. inermis* as the most common species. *Corbisema camera* and *C. triacantha* may also be present. The general silicoflagellate diversity is low relative to superjacent zones. *Pseudonaviculopsis* morphologies can occur near the top of this zone.

OCCURRENCE: This zone is present from the bottom of the study interval in Hole 208 up through ~554.0 mbsf and occurs in Hole 700B (Ciesielski 1991) from the base of the siliceous interval at 301.4 mbsf up through ~297.6 mbsf.

***Pseudonaviculopsis dissymmetrica* Acme Zone**

DEFINITION: Interval from the base (FCO) of the *Pseudonaviculopsis dissymmetrica* acme to FO *Dictyochoa precarentis*.

AUTHORS: McCartney, Witkowski and Szaruga (this report).

ASSEMBLAGE: This interval contains abundant *Pseudonaviculopsis* in addition to the various *Corbisema* species that are characteristic of the lower zone. While *Pseudonaviculopsis dissymmetrica* is the primary indicator for this zone, the Hole 208 acme observed beginning at ~554.0 mbsf includes abundant specimens of *Pseudonaviculopsis constricta*, which is considered a secondary zonal indicator. *Pseudonaviculopsis constricta* may be applicable as a zonal indicator where *Ps. dissymmetrica* is less abundant, as occurs in northern mid-latitude sites (Locker and Martini 1987).

REMARKS: This zone has abundant and often dominant skeletons of the robustly constructed (crenulate) *Ps. dissymmetrica* and the gracile *Ps. constricta*. Dumitrică (1973) reported a three-sided morphology with crenulate elements, which Ling (1981) used as a biostratigraphic marker. We observed this morphology, identified here as *Corbisema inermis crenulata*, to be uncommon.

OCCURRENCE: In Hole 208, we identify the base of this zone at ~554.0 mbsf with *Pseudonaviculopsis* morphologies observed to uncommonly occur further down the core (Table 2). In Hole 700B, the zone occurs from ~297.62 to ~295.15 mbsf (Table 7).

***Dictyochoa precarentis* Partial Range Zone**

DEFINITION: Interval from the FO *Dictyochoa precarentis* to FCO *Naviculopsis constricta*.

AUTHORS: McCartney, Witkowski and Szaruga (this report). A zone by the same name described in Ciesielski (1991) has different definitions for both the base and top.

ASSEMBLAGE: *Dictyochoa precarentis* is often the dominant taxon in this zone, although this tends to diminish in abundance in the interval that includes *N. primitiva*. Other abundant species include *C. camera*, *C. hastata* (various subspecies), *C. inermis*, *C. triacantha*, *Ps. constricta* and *Ps. dissymmetrica*.

OCCURRENCE: This zone extends to the base and likely below the studied intervals in Holes 752A and 1121B. FO *D. precarentis* is recorded at ~550.25 mbsf in Hole 208 and ~295.15 mbsf in Hole 700B (Table 7).

Within *Dictyochoa precarentis* Zone we identify four subzones defined by the presence of *Naviculopsis primitiva* and *N. cruciata*. The subzones are not recognized in Hole 1121B, where none of the subzonal markers are observed.

***Dictyochoa precarentis* Subzone**

DEFINITION: Interval from the base of the *D. precarentis* Zone to FCO *N. primitiva*.

AUTHORS: McCartney, Witkowski and Szaruga (this report).

REMARKS: This subzone includes a general abundance of *D. precarentis*. The presence and relative abundance of *Pseudonaviculopsis* species varies with location, being abundant in Hole 208 but generally not present in Hole 752A.

***Naviculopsis primitiva* Subzone**

DEFINITION: Interval from FCO to LO *Naviculopsis primitiva*.

AUTHORS: McCartney, Witkowski and Szaruga (this report).

REMARKS: *D. prearentis* and *Pseudonaviculopsis* spp. are nearly entirely absent in the interval, in which *N. primitiva* is present in Holes 700B and 752A.

***Naviculopsis cruciata* Subzone**

DEFINITION: Interval from the LO *Naviculopsis primitiva* to LO *Naviculopsis cruciata*.

AUTHORS: McCartney, Witkowski and Szaruga (this report).

REMARKS: In Holes 700B and 752A, *N. cruciata* appears immediately above the acme of *N. primitiva*. *Pseudonaviculopsis* spp. are generally not observed in association with *N. primitiva*, but do co-occur with *N. cruciata*.

***Pseudonaviculopsis constricta* Subzone**

DEFINITION: Interval from LO *Naviculopsis cruciata* to FCO *Naviculopsis constricta*.

AUTHORS: McCartney, Witkowski and Szaruga (this report).

REMARKS: This subzone was observed in Holes 700B and 752A, where *Ps. constricta* is consistently the most abundant species of *Pseudonaviculopsis*. Hole 1121B lacks *N. primitiva* and *N. cruciata*, with an inconsistent predominance of *Ps. constricta* among *Pseudonaviculopsis*, and thus subzones could not be identified in that hole.

***Naviculopsis constricta* Partial Range Zone**

DEFINITION: Interval from the FCO *Naviculopsis constricta* to FCO *Naviculopsis foliacea*.

AUTHORS: Bukry and Foster (1974), modified in Bukry (1977b).

ASSEMBLAGE: Besides *N. constricta*, other species that commonly occur throughout the span of the zone are *C. apiculata*, *C. hastata* and *C. triacantha*. *Dictyocha prearentis* is abundant in the lower portion and *N. eobiapiculata* becomes abundant in the middle portion of the zone.

INTERVAL: The base of this zone occurs at ~236.3

mbsf in Hole 752A, ~272.2 mbsf in Hole 700B, and ~39.1 mbsf in Hole 1121B. While a few specimens were tentatively identified as *N. foliacea* in Hole 752A, these were not common or consistent enough to suggest that the superjacent zonal boundary had been reached.

Calibration of silicoflagellate datums to GTS2012

In order to place the silicoflagellate datums outlined above in a global chronostratigraphic context, we have calibrated the age for each nannoplankton zone (NP) and silicoflagellate bioevent at each site considered here to GTS2012. Depths and the associated ages are listed in Tables 1 and 7, respectively.

FCO *Ps. dissymetrica* acme is consistently observed within upper calcareous nannofossil zone NP4. The interpolated age is ~62.06 Ma in Hole 208 and ~61.96 Ma in Hole 700B. These ages are remarkably consistent; the ~100 thousand year (kyr) difference may result from the lack of nannofossil tie points in the basal part of the siliceous microfossil-bearing interval in Hole 700B.

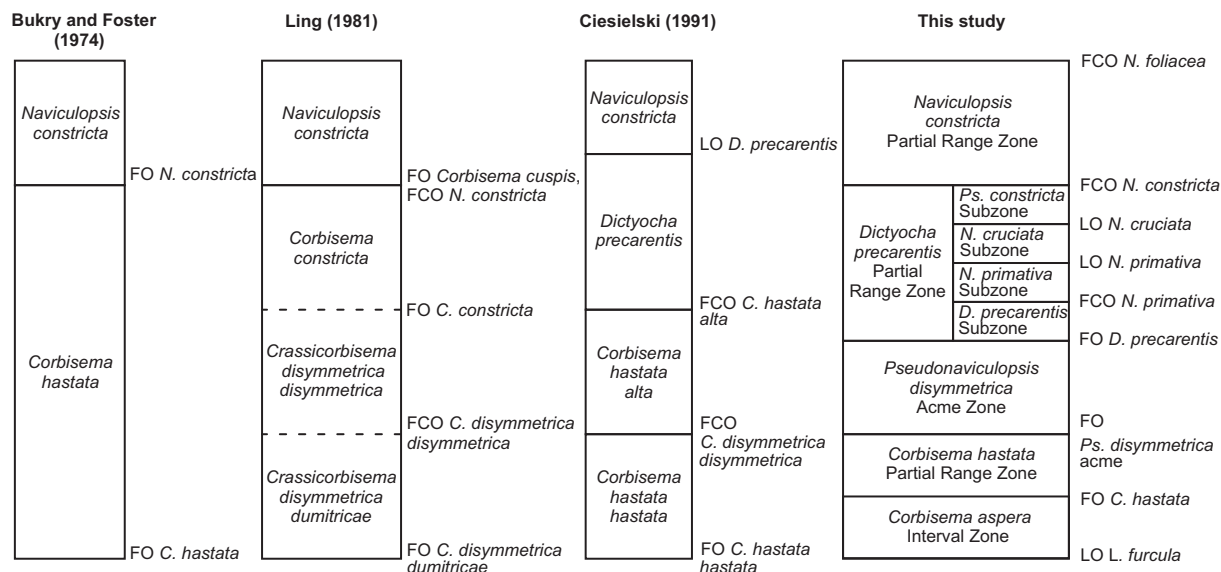
FO *D. prearentis* is also observed only in Holes 208 and 700B, but with a larger temporal discrepancy. This datum is observed within uppermost NP4 nannofossil zone (~61.66 Ma) in Hole 700B and basal NP5 (~61.44 Ma) in Hole 208.

FCO *N. primitiva* is placed at various levels within calcareous nannofossil zone NP5 at Holes 208, 700B and 752A (Table 7). Interpreted age varies within a ~300 kyr range, from 60.2 Ma (upper NP5) in Hole 752A to uppermost NP5 with ages of ~59.94 and ~59.72 Ma, respectively, in Holes 700B and 208.

The interpreted age of LO *N. primitiva* varies within a range of ~50 kyr. In Holes 752A and 700B, we estimate the age of this datum at ~59.78 and ~59.74 Ma (uppermost NP5 zone), respectively.

LO *N. cruciata* is observed within uppermost NP5 zone in Holes 700B (~59.68 Ma) and 752A (~59.62 Ma). Estimated age varies by ~<100 kyr, which makes this a remarkably consistent silicoflagellate datum.

FO *N. constricta* is the least consistent of the bioevents considered here, with age that varies by as much as ~1.5 million years (myr), from mid-NP6 through upper NP8 calcareous nannofossil zones (Table 7). The estimated age is ~59.21 Ma in Hole 752A, ~58.68 Ma in Hole 700B, and ~57.75 Ma in Hole 1121B.



Text-fig. 4. Comparison of the Palaeocene–Eocene silicoflagellate biostratigraphic zonation proposed here to previous southern subtropical to subpolar zonal schemes

INTERPRETATION AND DISCUSSION

Despite a wealth of literature, previous fossil silicoflagellate studies have largely dealt with individual localities, or a drilling leg of several sites in a region. Systematic studies focused on specific intervals of geologic time over a wide portion of the globe have been rare. Much of the previous deep sea silicoflagellate study dates to the DSDP era, which is often ambiguous due to fragmentary recovery; also taxonomic and biostratigraphic concepts have since undergone considerable refinement. This paper provides focus on a temporally limited and poorly known portion of the Cenozoic record using cores from a large area of southern mid- and high-latitude oceans and provides numerical ages to allow comparison of the timing of bioevents, which represents a major step forward in the development of Palaeogene silicoflagellate biostratigraphy.

Comparison to previous zonations

Previous silicoflagellate biostratigraphic zonations for the Palaeocene (Text-fig. 4) reflect developing understanding of silicoflagellate evolution over the past fifty years. The first Palaeocene silicoflagellate zonation (Bukry and Foster 1974) has two zones that represent the genera *Corbisema* and *Naviculopsis* then known from the epoch. Glezer (1979; revised in

Kim and Glezer 2007) also proposed a zonation based on two *Corbisema* species. The four-sided *Dictyochoa* morphology was not known to occur abundantly in the Palaeocene until the description of *D. prearentis* by Bukry (1976). The large two-sided morphologies here placed in *Pseudonaviculopsis* gen. nov. have been known since Dumitrică (1973), but were for the most part retained within *Corbisema*, the exception being the crenulated three- and two-sided morphologies that Ling (1981) placed into *Crassicorbisema* and then used biostratigraphically. Ciesielski (1991) proposed the first Palaeocene zonation that utilized *D. prearentis*. Neither *Naviculopsis cruciata* nor *N. primitiva*, however, both of which were described by Ciesielski (1991), were used in biostratigraphy prior to the present study.

Bukry and Foster (1974) proposed FO *Corbisema hastata* as the zonal marker for the lowest silicoflagellate zone of the Palaeogene. FO *Naviculopsis constricta* was proposed as the zonal marker for the base of the superjacent zone, which extended into the lower Eocene. This partition of the Palaeocene into two silicoflagellate zones has seen wide use (Bukry 1973, 1975, 1976, 1977b, 1981; Busen and Wise 1976; Locker and Martini 1987; Tsoy 2011), but offers a limited stratigraphic resolution. Glezer (1979) also used *C. hastata* as well as *C. lamellifera*, but this zonation is largely based on fossils from the Eurasian platform, and has seen little utility in deep sea sites.

The Glezer (1979) zonation is not discussed further in this study.

Ling (1981) replaced Bukry's *Corbisema hastata* Zone with *Crassicorbisema disymmetrica dumitricae*, *C. disymmetrica disymmetrica* and *Corbisema constricta* zones. The genus *Crassicorbisema* described by Ling (1981) and used for two of his zones included two and three-sided skeletons of massive construction that excluded two-sided morphologies of generally similar size but gracile design, such as *C. constricta*. The genus *Crassicorbisema* has generally not been recognized by subsequent workers (Locker and Martini 1987; Ciesielski 1991; Dumitrica 2014), and Ling's (1981) zonation has not been subsequently utilized. In this paper, we place the large two-sided skeletal morphologies whose evolution predates *Naviculopsis* into the new genus *Pseudonaviculopsis*, but retain three-sided skeletons with similar ultrastructures in *Corbisema* (see discussion in Systematic Palaeontology section, below).

Ciesielski (1991) proposed a zonation that included the *C. hastata* and *N. constricta* zones although defined differently than by Bukry and Foster (1974), and inserted between these two additional zones, separated in order of occurrence by LCO *C. hastata alta* and LO *D. prearentis*. Neither of the additional zones, as described by Ciesielski, have been subsequently used. Our observations are that *C. hastata alta* shows considerable variation and identification can be subjective, and the LO *D. prearentis* is also subjective. We also find the *Pseudonaviculopsis* acme to be distinct and widespread in southern latitude sites.

This paper builds on elements of all of the above zonations, using as zonal markers FO *C. hastata*, FCO *Ps. disymmetrica* acme, FO *D. prearentis* and FCO *N. constricta*. One useful consequence of this zonation is that each zonal bioevent is the first morphotypic common occurrence in the Cenozoic. Our zonation is partly based on short-ranging taxa, which have a considerable potential for high-resolution age control. The *D. prearentis* Zone is subdivided into subzones in Holes 208, 700B and 752A, but subzonal markers were not observed in Hole 1121B, possibly due to a missing sediment interval. Should future deep sea drilling recover new noncalcareous Palaeogene sequences in the Southern Ocean, the zonation proposed here can be tested and further refined.

Diachroneity in silicoflagellate datums

This work deals with Palaeocene sites located along a ~30° palaeolatitudinal transect (Text-fig. 1B) and the silicoflagellate biostratigraphy presented

here could potentially be biased by diachroneity in calcareous nannofossil datums. Keeping this caveat in mind, the age calibrations put forward in this study are remarkably consistent, with five of the six silicoflagellate datums varying between individual sites by less than 300 kyrs. Furthermore, the interpolated ages of two bioevents (FCO acme *Ps. disymmetrica* and LO *N. cruciata*) differ between sites by ~100 kyrs, which should be considered as within the age model error range.

The only unambiguous case of diachroneity identified in this study is FCO *N. constricta*. The age of this silicoflagellate datum differs between Holes 752A (~49°S at 58 Ma) and Hole 1121B (~73°S at 58 Ma) by as much as 1.46 myr (~59.21 versus ~57.75 Ma, respectively). This could be due to palaeobiogeographic reasons, with *N. constricta* originating in mid-southern latitude waters, and then migrating to the southern subpolar region. This scenario would imply a considerable palaeobiogeographic disparity in early Palaeogene silicoflagellate assemblages, which would be against the widespread belief of little palaeobiogeographic provincialism in early Palaeogene oceans (e.g., Lazarus *et al.* 2014). Other potentially diachronous Palaeogene silicoflagellate datums (e.g., *Dictyocha hexacantha*; Barron *et al.* 2015), and the reasons for their diachroneity, remain to be examined, and are likely to make a considerable impact on the existing silicoflagellate biostratigraphic zonations, and our understanding of the Palaeogene marine plankton palaeobiogeography.

Observed silicoflagellates of particular interest

Besides the above zones, four sediment intervals identified in this study are of particular interest in terms of silicoflagellate evolutionary history. These are, from oldest to youngest: (1) acme of two-sided silicoflagellate morphologies in Hole 208; (2) early evolution of *Naviculopsis* as observed in Hole 752A; (3) occurrence of unusual silicoflagellate morphologies that include two new species in Hole 752A; and 4) a narrow interval in Hole 524 that includes *N. danica*. These four intervals, each of which requires further study, are summarized below.

This study provides the first detailed assemblage data for the silicoflagellate-bearing interval from the early and middle Palaeocene of Hole 208. Large two-sided silicoflagellate morphologies here placed in the new genus *Pseudonaviculopsis* range throughout this interval, but an abundance acme is used to define the base of *Ps. disymmetrica* Zone. This acme includes considerable skeletal diversity in the structure of the

basal rings and pikes, with common teratoid specimens. High abundances of these morphologies in Hole 700B suggest the duration of this zone from ~61.96 to ~61.66 Ma, which is largely consistent with Site 208.

Naviculopsis primitiva occurs in Hole 752A between ~60.20 and ~59.78 Ma, immediately preceding a short interval of *N. cruciata* (~59.78 to ~59.62 Ma) and postdating the common occurrence of *C. hastata alta* (Table 5; see also Ciesielski 1991). In this study, Hole 700B was examined at a higher resolution than in Ciesielski (1991), and shows *N. primitiva* to occur between ~59.94 and ~59.74 Ma, and *N. cruciata* between ~59.74 and ~59.68 Ma, with *C. hastata alta* present just below the FO *N. primitiva* (Table 4; Ciesielski 1991). Although the ages are slightly different, the sequence of bioevents is consistent with Hole 752A, documenting an evolutionary transition from the *C. hastata alta* morphology with a short minor-axis side to a *Naviculopsis* basal ring that has an apical structure with three struts (*N. primitiva*) and four struts with a short bridge (*N. cruciata*). We agree with Ciesielski (1991) that this represents the divergence of *Naviculopsis*.

Neither *N. primitiva* nor *N. cruciata* were observed in Hole 1121B. These species may not have occurred at that high southern latitude or – alternatively – may have not been detected in this study due to considerable recovery gaps within cores 1121B-11X and -12X (Text-fig. 3).

The youngest interval of Hole 752A studied here, dated at ~54.18 to ~53.87 Ma, includes several silicoflagellates previously not reported from the deep sea. This interval includes the new species *Dictyochoa castellum* and *Stephanocha? fulbrightii*, both of which are extraordinary: *D. castellum* for the presence of eight secondary spines on the basal ring and *S.? fulbrightii* for an early appearance of ringed and multi-windowed apical structures. Specimens of both new species are rare, but distinctive enough to potentially become useful zonal markers, should future drilling in the Indian Ocean recover correlative intervals.

Hole 524 represents a short siliceous interval from which relative diatom counts were reported by Gombos (1984) and Fenner (1991). We examined for silicoflagellates the two samples studied by Gombos (1984) (dated at ~56.89 to ~56.50 Ma), and these show an assemblage from the *Naviculopsis constricta* Zone that includes the first known occurrence in southern latitude sites of the unusual species *N. danica*. This species was previously known only from northern mid-latitude sites (Perch-Nielsen 1976; Bukry 1978b).

SYSTEMATIC PALAEOONTOLOGY

McCartney and Witkowski (2016) provide a detailed discussion of Cenozoic silicoflagellate skeletal terminology, which is followed here. The proportional length of the basal spines is in comparison to the distance across the basal ring along the same axis. The synonymies below generally include only the first description and additional references that show the history of classification. LM micrographs are shown in Plates 1–3; SEM micrographs in Plate 4.

Class Dictyochoephyceae Silva, 1980

Order Dictyochoales Haeckel, 1894

Family Dictyochoaceae Lemmermann 1901

Genus *Corbisema* Hanna, 1928

Corbisema apiculata (Lemmermann) Hanna, 1931
(Pl. 2, Fig. 7, double skeleton; Pl. 4, Fig. 6)

1901. *Dictyochoa triacantha* var. *apiculata* n. var.; Lemmermann, p. 259, pl. 10, figs 19, 20.

1931. *Corbisema apiculata* (Lemmermann) n. comb.; Hanna, p. 198, pl. D, fig. 2.

REMARKS: *Corbisema apiculata* was originally proposed based on material from Fur, Denmark. Lemmermann's (1901, p. 259) description reads (our annotations in square brackets): “supporting spines [pikes] 14 µm long, with hook-shaped ending [pointing] to the inner side and tapering to a thin tip”. Lemmermann (1901, fig. 20) illustrated one of these, also from Fur, in oblique lateral view that shows precisely these morphological features for the pikes. Schulz (1928, fig. 29a) illustrated skeletons of *C. apiculata* in an oblique apical view that also shows prominent pikes pointing abapically, consistent with Lemmermann's description and illustrations. Both Lemmermann's and Schulz's taxonomic concepts were corroborated by our observations from Fur materials (McCartney *et al.* 2015b, pl. 1, figs 4–8; see also Tsutsui *et al.* 2018). However, other workers have applied the name *C. apiculata* to skeletons with equilateral triangular basal rings bearing short corner spines, without regard to pike length or orientation (Bukry 1975; Ciesielski 1991), or to skeletons with no pikes (Busen and Wise 1976). This has resulted in a broadly interpreted species that ranges from the Late Cretaceous (McCartney *et al.* 2011b) to early (Bukry 1975; Shaw and Ciesielski 1983) or late Oligocene (Bukry 1976; Busen and Wise 1976).

The pikes of *C. apiculata* are most typically lo-

cated beneath the strut attachment, but can be offset and such unusual morphologies occur from the Cretaceous (Perch-Nielsen 1975, pl. 2, fig. 16) to the early Eocene (McCartney *et al.* 2015b, pl. 2, fig. 3). McCartney *et al.* (2015a, b and Tsutsui *et al.* 2018) suggested that such prominent pikes in this orientation may serve to support the cell boundary of the paired skeleton in the Star-of-David configuration. Double skeletons that exhibit such prominent pikes occur for *C. apiculata* (Schulz 1928, fig. 27; McCartney *et al.* 2015a), *C. hastata* (McCartney *et al.* 2014a) and *C. archangelskiana* (Schulz 1928, fig. 75; McCartney *et al.* 2010a, 2015a), all in the Star-of-David configuration. Such prominent pikes become notably less abundant among silicoflagellates after the middle Eocene.

In this paper, we restrict the identification of *C. apiculata* to skeletons that have a medium-sized (~40 µm) equilateral basal ring and prominent pikes that point abapically. This interpretation considerably changes the perceived abundance of the species and replaces *C. glezeriae* (Bukry 1976), used by Ciesielski (1991) for the late Palaeocene. Silicoflagellates similar to *C. apiculata* that either lack or have only small pikes are in this paper included in *C. camera* Ciesielski, 1991 as emended below to provide a somewhat broader species concept to include skeletons that have pikes and may have a lower apex.

This interpretation also changes the FO of the species, since the oldest known specimen of *Corbisema*, identified as *C. apiculata* by McCartney *et al.* (2011b), does not appear to have prominent pikes. Specimens identified as *C. apiculata* that do have prominent pikes are found in the Cretaceous (McCartney *et al.* 2011a) but whether these are consistent with those from the early Cenozoic will require further study; these could possibly be included in *Corbisema trigona*, described from the Late Cretaceous. We tentatively apply *Corbisema cf. trigona* to some medium-sized skeletons observed in Hole 208 with linear sides, small pikes and a low apex, and are searching for material from the type locality (Coesfeld, North Rhine-Westphalia, western Germany) in order to examine the type material.

Corbisema archangelskiana (Schulz) Frenguelli, 1940
(Pl. 1, Fig. 4, four-sided variant)

1928. *Dictyocha triacantha* var. *archangelskiana* n. var.; Schulz, pp. 250, 251, figs 33a–c, 77, 78.

1940. *Corbisema archangelskiana* (Schulz) n. comb.; Frenguelli, fig. 12a.

REMARKS: The Late Cretaceous and Palaeocene show a diversity of extraordinarily large silicoflagellates that generally lack basal spines, including *Corbisema archangelskiana* and *C. inermis*. Both species display considerable variability, including pikes of various lengths and shapes. There is, however, much confusion in the identification of these two taxa in the literature, caused in part by the wide range of morphologies illustrated by Schulz (1928) with his original description of *C. archangelskiana*; Lemmermann (1901) provided a single illustration of *C. inermis* that had prominent pikes, which were not shown in Schulz's (1928) illustrations. Some workers have exclusively used *C. archangelskiana* for the Cretaceous (see McCartney *et al.* 2011a), while others (Bukry 1976; Locker and Martini 1987) have only applied *C. inermis* to Cenozoic forms. Ciesielski (1991) identified both morphologies in the upper Palaeocene of Hole 700B, with which we concur.

Corbisema archangelskiana often has blunt to squared corners with the sides more inflected towards the middle of the basal plane in a cloverleaf shape, with short struts when seen in apical view, while *C. inermis* has a rounder basal ring and longer struts (compare Glezer 1966, pl. 8, figs 1–5 and figs 6, 7). The measure that we generally used to differentiate between these taxa is that for *C. inermis*, the struts are of a length that would nearly reach to the corners, while for *C. archangelskiana*, the distance in apical view from apex to corner is more than 1.5 times the length of the struts. The use of these ratios is consistent for the specimens illustrated by Lemmermann (1901), Schulz (1928) and Glezer (1966).

The wide range of variation present in *C. archangelskiana* and *C. inermis* needs more thorough study. Members of this group of large three-sided morphologies have rounded basal corners and short or absent spines but the presence and lengths of pikes vary widely and deserve especially careful examination. This is especially important in light of the observation presented in the next taxon, *C. aff. archangelskiana*, that double skeletons of this group apparently occur in both the Star-of-David and corner-aligned configurations. More study is needed to better delineate, or redescribe, *C. archangelskiana* and *C. inermis*, combined with observations of additional double skeletons.

Occasional examples of large quadrate skeletons that lack corner spines are listed in Tables 2, 4 and 5. While Ciesielski (1991) considered similar morphologies from the middle Palaeocene of Hole 700B

as *Dictyochoa* spp., we argue the early age and rarity of these morphologies suggests these to be varieties of a large *Corbisema* such as *C. archangelskiana*. Ciesielski (1991) identified a single specimen as *C. cf. flexuosa* (Stradner) Perch-Nielsen, 1975, noting that the morphology lacked the apical plate and was older than previously known specimens. In this study, three observed specimens of similar morphology are included in *C. archangelskiana*.

Corbisema aff. *archangelskiana* (Schulz)

Frenguelli, 1940

(Pl. 1, Figs 2, 3)

REMARKS: Skeletons of size comparable to the co-occurring *C. archangelskiana* with rounded but slightly pointed corners and short pikes (Pl. 1, Fig. 2) occur between 142.5 and 127.2 mbsf in Hole 752A (Table 5). These would have been placed within the range of variation of *C. archangelskiana* but for the observation of a slightly disarticulated double skeleton (Pl. 1, Fig. 3) where the two skeletons appear to have separated from a corner-aligned configuration. This specimen does appear to be a true doublet, as the two individual skeletons are similar and each has an apex that points away from the other. Two double skeletons of large *Corbisema* without basal spines, both in the Star-of-David configuration are known, including one that came from 231.14 mbsf in Hole 752A (see McCartney *et al.* 2015a, fig. 7D). The observation of a generally similar morphology that was likely in the corner-aligned configuration suggests that this silicoflagellate is not directly related to *C. archangelskiana*. Indeed, McCartney *et al.* (2015a) present the hypothesis that the two double skeleton configurations may represent separate evolutionary lineages and in such a case should be interpreted as separate genera.

The evidence presented here is not definitive, since the double skeleton is slightly disarticulated. However, this observation further demonstrates how little we know about the early Cenozoic evolution of the three-sided skeletal morphologies. Several of the often used *Corbisema* species, including *C. archangelskiana*, *C. hastata* and *C. triacantha* have enough range of diversity to suggest that multiple biologic species can have similar skeletal designs. The apparent occurrence of *archangelskiana*-like double skeletons in both configurations suggests this skeletal morphology may be polyphyletic. Such a conclusion could explain the observed wide range of pike lengths.

Corbisema bimucronata elegans Bukry, 1987

1950. *Corbisema bimucronata* n. sp.; Deflandre, pp. 63, 82, figs 174–177.

1987. *Corbisema bimucronata elegans* n. subsp.; Bukry, p. 405, pl. 3, figs 7–10.

REMARKS: The few specimens observed from Hole 752A have two closely spaced small spines on each tightly rounded corner.

Corbisema camera Ciesielski emend. McCartney, Witkowski and Szaruga

1991. *Corbisema camera* n. sp.; Ciesielski, pl. 4, figs 3–6.

REMARKS: This ~30–40 µm silicoflagellate was described by Ciesielski (1991) as having a highly arched apical structure and robust skeletal elements. The description, however, does not indicate the presence or absence of pikes, although one of the two illustrated specimens (Ciesielski 1991, pl. 4, fig. 3, upper left side) appears to have a pike beneath the strut attachment. The basal ring size and shape of *C. camera* and *C. apiculata* are similar but our interpretation of the latter taxon (see above) includes prominent pikes that point abapically. We hereby emend the description of *C. camera* to include short pikes, usually located beneath the strut attachment, although pikes may be absent.

This interpretation thus combines *C. apiculata* and *C. camera* counted by Ciesielski (1991), which have a similar stratigraphic range in Hole 700B (see range chart in Ciesielski 1991). Ciesielski counted a larger proportion of *C. glezeriae* (included in *C. apiculata* in this study) than observed in Hole 752A in this study. However, we only counted a specimen as *C. apiculata* if the prominent pikes were evident and thus our numbers probably include some *C. apiculata* in apical view counted as *C. camera*.

Corbisema cunicula (Bukry) McCartney, Witkowski and Szaruga comb. nov. et stat. nov.

(Pl. 1, Fig. 8)

1976. *Corbisema hastata cunicula* n. subsp.; Bukry, p. 892, pl. 3, figs 8–15.

1991. *Corbisema triacantha lepidospina* n. subsp.; Ciesielski, pp. 77, 78, pl. 4, figs 9–14.

REMARKS: Two closely similar silicoflagellate subspecies, *C. hastata cunicula* and *C. triacantha*

lepidospinosa, with a ~20 µm basal ring and long spines occur in the late Palaeocene to early Eocene of Southern Hemisphere sites. We find these two morphologies to be difficult to distinguish and count the range of morphologies as a single taxon. The senior trinomial published by Bukry (1976) is given priority over that of Ciesielski (1991). However, the small size and long spines are distinct enough from co-occurring *C. hastata* and subspecies recognized in this study that we elevate *C. hastata cunicula* to species level as *C. cunicula*.

Basal ring morphologies that have one side slightly shorter than the other two (i.e., similar to *C. hastata*) predominate, but equilateral rings also occur, particularly in the *N. primitiva* Subzone. Basal diameters, measured as the length of the major axis, range from 10 to 25 µm and basal spine lengths can vary from half to greater than the basal diameter. Basal ring usually has major-axis sides that are slightly convex and a minor-axis side that is linear to slightly indented at the strut attachment. Pikes are short and may not be present, which is a feature different from most *C. hastata*. Specimens identified as *C. triacantha* in this study consistently had shorter basal spines.

Corbisema falklandensis Bukry, 1976

1976. *Corbisema falklandensis* n. sp.; Bukry, p. 891, pl. 2, figs 1–15.

1976. *Pseudomicromarsupium gombosum* n. sp. (an ebridian); Busen and Wise, Jr., p. 716, pl. 12, figs 1–6.

REMARKS: This species has an extraordinary skeletal structure, with robust teardrop-shaped basal ring, forked pikes and a size range from 50 to 70 µm across the basal ring major axis. This species uncommonly occurs over a wide stratigraphic interval in Holes 700B, 752A and 1121B. The *D. prearentis* Zone is the lowest in which this taxon was observed, which is consistent with observations by Ciesielski (1991).

This species can have unusual variability. We have observed several specimens that have various complex apical structures, including an apically ringed skeleton (46.46 mbsf in Hole 1121B), and a variant morphology with six struts (52.86 mbsf in Hole 1121B). Also counted in this taxon is an even more uncommon morphology that has pointed corners and large but non-forked pikes that could, with more study and higher specimen counts, deserve description as a separate species.

Corbisema hastata (Lemmermann) Frenguelli, 1940
s. ampl.

1901. *Dictyochoa triacantha* var. *hastata* n. var.; Lemmermann, p. 259, pl. 10, figs 16, 17.

1928. *Dictyochoa triacantha* var. *hastata* Lemmermann; Schulz, pp. 249, 250, fig. 31a, b.

1940. *Corbisema hastata* (Lemmermann) n. comb.; Frenguelli, p. 63, fig. 13c.

REMARKS: The name *C. hastata* has been applied to a range of silicoflagellate morphologies that have one basal side shorter than the other two, which results in a bilateral, rather than radial, symmetry. There is considerable variation of size and spine length in this group. We take as our species concept for *Corbisema hastata* the original illustrations of Lemmermann (1901) and Schulz (1928) that show a basal ring of arrowhead-shape, with the distance across the minor-axis corners being about half the distance from either of these to the major-axis corner. Both workers showed significant inflection of the minor-axis side at the strut attachment and prominent pikes whose terminations occur at some distance from the basal plane. The minor-axis basal spines generally point away from the region of the major-axis corner. In this study, we recognize several of the various subspecies distinguished within this taxon, and elevate one (*C. hastata cunicula*) to species level. Those skeletons similar to the original illustrations by Lemmermann (1901) and Schulz (1928), along with other hastatid morphologies that did not fit well elsewhere, were counted as *C. hastata s. ampl.*

Corbisema hastata alta Ciesielski, 1991
(Pl. 3, Figs 1–6)

1991. *Corbisema hastata* subsp. *alta* n. subsp.; Ciesielski, p. 75, pl. 4, figs 1, 2; pl. 9, fig. 10.

REMARKS: This taxon forms an acme at 280.05 mbsf in Hole 700B that appears to be a short-lived event. This acme was not observed in Hole 752A, although the abundance of *C. hastata alta* is high at 263.8 mbsf. This taxon shows considerable variability in the relative length and orientation of both the minor-axis side and spines. In some relatively uncommon specimens, the minor axis side is not perpendicular to the major axis, the associated corner spines are of uneven length, and the strut attachment on the minor side is often positioned slightly closer to the corner with the shorter basal spine. In this vari-

ant, the apical structure can have a slight rotation that is similar to specimens of *N. primitiva*. Based on this feature, Ciesielski (1991) considered this taxon to be the ancestor of *N. primitiva*, with which we concur.

Corbisema hastata globulata Bukry, 1976

1976. *Corbisema hastata globulata* n. subsp.; Bukry, p. 892, pl. 4, figs 1–8.

REMARKS: Compared to most *C. hastata* observed in this study, *C. hastata globulata* has major axis sides that are slightly convex, particularly near the minor-axis corners, and a minor-axis attachment that is not generally indented towards the middle of the basal ring. Spines point away from the middle region of the basal window and are usually considerably shorter than the portal diameter. Basal ring size tends to be larger (~40–50 µm) than most co-occurring members of the *C. hastata* group. As noted by Ciesielski (1991), this taxon ranges through most of the Palaeocene and is especially abundant in the upper Palaeocene.

Corbisema hastata minor (Schulz) Bukry, 1975

part 1928. *Dictyochoa triacantha* var. *apiculata* forma *minor* n. form; Schulz, p. 249, fig. 29b.

part 1928. *Dictyochoa triacantha* var. *hastata* Lemmermann; Schulz, p. 249, fig. 31c.

1975. *Corbisema hastata minor* (Schulz) n. subsp.; Bukry, p. 854, pl. 1, fig. 10.

REMARKS: The two major-axis sides of this skeletal morphology curve near the connections to the minor-axis side, which can be nearly linear to slightly indented at the strut attachment. The two minor-axis spines generally point away from some point that would be beyond the opposite major-axis corner, and may in some cases be nearly parallel to one another and roughly parallel to the major-axis.

Corbisema inermis crenulata Bukry, 1976

1976. *Corbisema inermis crenulata* n. sp.; Bukry, p. 892.

1991. *Corbisema disymmetrica crenulata* (Bukry) n. comb.; Ciesielski, p. 74, pl. 1, figs 1, 2.

REMARKS. See discussion below for *C. inermis inermis*. Both Dumitrică (1973) and Ling (1981) reported this taxon as abundant in Hole 208, in an inter-

val below the first appearance of *Pseudonaviculopsis disymmetrica*, and Ling has used this as the zonal marker for the *Crassicorbisema disymmetrica dumitricae* Zone. None of the samples examined here comprised abundant three-sided massively constructed forms; only occasional specimens were observed. This difference in abundance may have been caused by the use of unsieved residues in this study.

Corbisema inermis inermis (Lemmermann) Bukry, 1976

1901. *Dictyochoa triacantha* var. *inermis* n. var.; Lemmermann, pl. 10, fig. 21.

1976. *Corbisema inermis inermis* (Lemmermann) n. comb.; Bukry, p. 892, pl. 5, figs 1–3.

REMARKS: Lemmermann's (1901) description of this taxon is quite general, although his single illustration shows medium-sized pikes. A double skeleton figured by Schulz (1928, fig. 75) shows similar pikes that point towards the middle of the portals, the paired skeleton being in the Star-of-David configuration (McCartney et al. 2010a). This species is often difficult to distinguish from *C. archangelskiana*, since the basal ring shape and pike lengths for both taxa are quite variable. The method used to differentiate between these taxa is presented in the *C. archangelskiana* section above.

The *C. inermis* range of variation includes basal ring morphologies that have or may lack corner spines. Sediments from Site 208 yielded large skeletons of *C. inermis* with massively constructed ("crenulate") skeletal elements, here placed in *C. inermis crenulata*, that generally lack spines but two spined specimens were observed and are marked with "sp." in Table 2. Specimens with similar size and shape but without the massively built skeletal elements are here termed "gracile". The crenulate and gracile skeletal morphologies co-occur with *Pseudonaviculopsis* spp. discussed below, where the terms are similarly applied.

Ling (1981) placed the crenulate skeletons of this and the co-occurring two-sided taxon into the genus *Crassicorbisema*, while the gracile morphologies were retained in *Corbisema*. We observe crenulate and gracile morphologies with three basal sides that have similar ranges of variability that does not suggest separation into two genera, and count the crenulate and gracile skeletons as subspecies of *C. inermis*. For example, five three-sided specimens with similar basal shape and size, and prominent corner spines, were observed at 550.5 mbsf in Hole 208. Four of these were of the gracile morphology and one crenu-

late. The general similarities of these skeletons, aside from the thickness of the skeletal elements, suggest to us that all five skeletons are ecophenotypic variants of the same species. Similarly overbuilt skeletons occur in other not-directly related silicoflagellates of middle Eocene age (Witkowski *et al.* 2012).

Corbismea inermis minor (Glezer) Bukry, 1976

1966. *Dictyochoa triacantha* var. *inermis* f. *minor* n. form; Glezer, p. 247, pl. 8, figs 3–5; pl. 31, fig. 7.

1976. *Corbisema inermis minor* (Glezer) n. comb; Bukry, p. 892, pl. 5, figs 4–7.

REMARKS: This taxon has a small, nearly round basal ring, with relatively thick basal elements. The size range reported for this taxon by Glezer (1966) is 15–30 μm across the sides; specimens illustrated by Bukry (1976) are in the upper end of this range. The taxon was observed to have a long range, through calcareous nannofossil zones NP3 and NP4 in Hole 208 and NP5 to NP8 in Hole 1121B. A few specimens have somewhat more pointed corners with small spines.

Corbisema triacantha (Ehrenberg) Hanna, 1931
s. ampl.

1931. '*Corbisema triacantha* (Ehrenberg)' n. comb.; Hanna, pl. D, fig. 1.

REMARKS: We follow Ciesielski's (1991; see also Bukry 1976) broad species concept for this taxon, which is characterized by small size, with small or absent pikes. The stratigraphic range of *C. triacantha* extends into the middle Miocene (Bukry 1982). A detailed SEM study is required to determine whether this is a species complex rather than a single species. The subspecies previously described as *C. triacantha lepidospina* is here placed in *C. cunicula*.

Corbisema cf. trigona (Zittel) Hanna, 1928
(Pl. 1, Figs 1, 5)

1876. *Dictyochoa trigona* n. sp.; Zittel, p. 83, pl. 2, fig. 6.

REMARKS: A large *Corbisema* with straight sides, corner spines and a low apex is present in Hole 208, particularly between 556.0 and 548.5 mbsf. This morphology has usually been identified as *C. apiculata* (for example, see McCartney *et al.* 2011b, pl. 5, fig.

7), but is inconsistent with the narrowed interpretation of *C. apiculata* used in this paper. We suggest an identification as *C. trigona* based on a single specimen of Late Cretaceous age from Coesfeld, North Rhine-Westphalia, western Germany, illustrated by Zittel (1876) and believed at that time to be a radiolarian. Zittel's (1876) specimen has an equilateral shape and measures 75 μm across the basal side ("arm" in Zittel 1876), which would be 65 μm from the basal corner to the opposite strut attachment, with spines of 8 μm . This is a close match to the specimen from McCartney *et al.* (2011b). The specimens observed in this study are of a slightly smaller size (~45–60 μm). Apical structure is low and pikes are generally absent.

Genus *Dictyochoa* Ehrenberg, 1839

Dictyochoa cf. byronalis Bukry in Barron *et al.*, 1984
(Pl. 4, Fig. 7)

1984. *Dictyochoa byronalis* n. sp.; Bukry in Barron *et al.*, p. 151, pl. 3, figs 1–14.

1987. *Dictyochoa* sp. cf. *D. byronalis* Bukry; Bukry, p. 398, pl. 6, fig. 5.

1991. *Dictyochoa cf. byronalis* Bukry; Ciesielski, pp. 64, 78, pl. 7, figs 5, 6.

REMARKS: Skeletal morphologies essentially identical to *Dictyochoa precarentis* though often of larger size (~50–80 μm) were observed from 154.40 to 126.23 mbsf in Hole 752A and were generally counted as *Dictyochoa precarentis s. ampl.* (see below). Among this group, however, are specimens with apical structure slightly rotated sinistrally when seen from apical view, which were counted as *Dictyochoa cf. byronalis*. Bukry (1987) similarly identified this morphology in the early Eocene and Ciesielski (1991) reported a single specimen from the middle Eocene. We consider these to be ancestral to *D. byronalis*, which are abundant in the middle Eocene Kellogg Shale (Barron *et al.* 1984, 2015), and to represent the divergence of the silicoflagellate lineage with sinistrally rotated apical structure that ultimately led to the evolution of *Distephanopsis crux* and *Stephanocha speculum* (see McCartney *et al.* 2014b).

Dictyochoa castellum McCartney, Witkowski and
Szaruga sp. nov.
(Pl. 2, Figs 1–3)

DESCRIPTION: Basal ring is essentially square be-

tween the corners with short corner spines. Between the basal corner and strut attachment, at a location usually closer to the attachment, is a usually larger secondary spine. Thus each basal side has four elements, and the skeleton usually has eight secondary spines, although some secondary spines may not occur. The four struts are relatively long and the apical bridge is short.

REMARKS: Specimens are rare, with only seven observed in more than 30 slides from three samples. A silicoflagellate that has a basal ring with similar secondary spines occurs in the late Pliocene (see *D. perlaevis ornata* Bukry, 1977b), but has a more rhomboid shape and considerably longer bridge. See McCartney and Wikowski (2016) for a short discussion on the occurrence of secondary spines.

OCCURRENCE: Specimens observed from 133.51 to 128.0 mbsf in Hole 752A, Broken Ridge, Eastern Indian Ocean.

HOLOTYPE (Pl. 2, Fig. 2): Sample 121-752A-14X-4, 49–50 cm (SZCZ #24260 slide X; note, this is the same slide that includes the type specimen for *S. fulbrightii*). Specimen is 77 μm across the triple junctions of opposite basal corners.

REPOSITORY: Institute of Marine Sciences, University of Szczecin Diatom Collection, Szczecin, Poland (SZCZ).

NAME DERIVATION: The name derives from the Latin word for “fortress” and is named for the resemblance between the basal ring outline and a Medieval bastion (star) fort, or *trace italienne*, design.

Dictyocha precarentis Bukry, 1976
(Pl. 1, Fig. 7)

1976. *Dictyocha precarentis* n. sp.; Bukry, p. 894, pl. 6, figs 6–13; pl. 7, figs 1–3.

REMARKS: This is the geologically earliest known species of *Dictyocha*, being abundant in the middle to late Palaeocene of Hole 752A. The FO *D. precarentis* is at 550.0 mbsf in Hole 208; specimens are usually ~25 μm across opposite basal corners, and the apical structure and flat sides of the basal ring with ~8 μm long spines are consistent with some of the co-occurring *C. triacantha*, which we consider as the ancestral species. *Dictyocha precarentis* is more abun-

dant and has longer spines (~15 μm) at 549.0 mbsf in Hole 208. At this level, *D. precarentis* skeletons have sides that are more indented at the strut attachments. Stratigraphically higher skeletons from the middle Palaeocene have small (<25 μm) to medium (<40 μm) size, with square basal ring, longer spines and short bridges. Struts attach approximately to the middle of each side, with small pikes beneath strut attachments or nearby.

At 221.97 mbsf in Hole 752A, 23 specimens of slightly smaller size and shorter spines were observed. These are considered to fall within the range of variation of *D. precarentis*. Variants of *D. precarentis* with a wider plate-shaped bridge were tabulated separately for Hole 1121B and were occasionally observed, but not separately tabulated in Hole 752A, especially at 221.97 mbsf. Some five-sided variants are listed separately for Holes 752A and 1121B.

Dictyocha precarentis is consistently present in Hole 752A between 253.7 and 211.66 mbsf. This apparent extinction was used as the marker for the top of the *Dictyocha precarentis* Partial Range Zone as applied by Ciesielski (1991). However, an essentially identical morphology (Pl. 1, Fig. 7) here listed as *D. precarentis s. ampl.* is observed higher in Hole 752A, from 144.7 mbsf to the top of the studied interval. This pattern of two separated *D. precarentis* intervals is also reported by Bukry (1976) from Hole 327A. *Dictyocha precarentis s. ampl.* has a greater range of variation, including larger sizes (> 60 μm) and sometimes a rhomboid rather than square basal ring. This taxon occurs over a similar stratigraphic range as *D. cf. byronalis*. The two morphologies together may represent the transition to *D. byronalis*, known from the middle Eocene (Barron et al. 1984; Bukry 1987; McCartney and Wise 1987; Ciesielski 1991; McCartney and Harwood 1992; Witkowski et al. 2012).

Genus *Naviculopsis* Frenguelli, 1940

Naviculopsis cf. americana Bukry in Barron et al.,
1984
(Pl. 1, Fig. 6; Pl. 4, Figs 4, 5)

1984. *Naviculopsis americana* n. sp.; Bukry in Barron et al., p. 151, pl. 4, figs 17–19; pl. 5, figs 1–5.

REMARKS: This taxon has a large basal ring (~70 μm across the major axis) with basal spines each measuring half or more of the basal ring diam-

eter. The basal sides can be linear or somewhat indented at the arch attachment. SEM micrographs show the basal side to sometimes narrow (Pl. 4, Fig. 5) in close proximity to the arch attachment when viewed abapically. The arch has a narrow band of width similar to the thickness of the basal elements that widens near the attachment (Pl. 4, Fig. 4). The taxon is consistently present from 144.7 to 135.8 mbsf in Hole 752A and was especially abundant (83 specimens in a single slide) at 142.50 mbsf (~54.15 Ma).

The specimens observed in this study are closely similar to those illustrated in Barron *et al.* (1984) but tend to be narrower across the minor axis. The specimens reported here, however, are considerably older than those from the Kellogg Shale, California, type locality of *N. americana* (~41 Ma, see Barron *et al.* 1984, 2015). Tsoy (2011, p. 95) reported this species to range from ~49 to ~34 Ma in Kamchatka, Russia.

Naviculopsis constricta (Schulz) *sensu* Bukry in Barron *et al.*, 1984

1928. *Dictyochoa navicula* var. *biapiculata* f. *constricta* n. form.; Schulz, p. 246, fig. 21.

1984. *Naviculopsis constricta* (Schulz) emend.; Bukry in Barron *et al.*, p. 151, pl. 5, fig. 6.

REMARKS: The basal ring of *N. constricta* is considerably longer across the major axis than along the minor axis. In lateral view, the arch attachment forms a broad pediment that, in apical view, gives the portals an elliptical shape.

Several specimens examined here had an apical band that made up about a third of the distance between the major axis corners. This is at the dividing point between *N. constricta* and *N. foliacea*, as defined by Bukry (1975). These are marked in Table 5 as *N. foliacea?* but considered to be in the range of *N. constricta* variation viewed in this study.

Naviculopsis cruciata Ciesielski, 1991
(Pl. 3, Figs 7–9; Pl. 4, Fig. 3)

1991. *Naviculopsis cruciata* n. sp.; Ciesielski, p. 83, pl. 9, figs 1–4, 5?.

REMARKS: See comments on *N. primitiva* below. This taxon has also been reported by Tsoy (2011) from the middle Eocene of Russia.

Naviculopsis danica Perch-Nielsen, 1976
(Pl. 1, Fig. 9)

1976. *Naviculopsis danica* n. sp.; Perch-Nielsen, p. 35, figs 5, 6, 21.

REMARKS: Eleven specimens of this taxon were observed in the two samples from Hole 524 (Table 3). The general structure is similar to *N. primitiva* but the basal ring is more rounded and one of the struts is often nearly perpendicular to the major axis. However, there is considerable variation and the apical structure can be rotated to an orientation closer to *N. primitiva* (see Perch-Nielsen 1976, fig. 21). *N. primitiva* and *N. danica* are separated temporally; the former occurs in calcareous nannofossil zone NP5 and the latter in NP9.

All previous reports of *N. danica* (Perch-Nielsen 1976; Bukry 1978b; Tsoy 2011) are from the Northern Hemisphere. Bukry (1976) lists a single specimen of *N. danica* within what we identify as the *D. pre-carentis* Zone at 71.8 mbsf in Hole 327A. Given the chronological differences between *N. primitiva* and *N. danica*, Bukry's (1976) report may represent *N. primitiva*.

Naviculopsis elongata (Glezer) McCartney,
Witkowski and Szaruga comb. nov.

1964. *Dictyochoa elongata* n. sp.; Glezer, p. 50, pl. 1, figs 5–7.

REMARKS: Glezer (1960, 1964, 1966) placed this skeletal morphology in *Dictyochoa* because she used that taxon rather than *Corbisema* for most three-sided silicoflagellates, and suggested this to be the transitional species between the three-sided silicoflagellates and *Naviculopsis*. This taxon was then only known from the early Eocene of Russia but has been subsequently observed in other locations, particularly in association with *N. danica* (Perch-Nielsen 1976; Bukry 1978b). The two taxa are closely similar, with an apical structure composed of three struts, one of these essentially parallel to the minor axis. *Naviculopsis elongata* differs in having a basal (corner) spine along the minor axis. As these taxa have close affinities we here formally transfer *D. elongata* as *N. elongata*.

Bukry (1978b) reported *N. danica* as considerably more abundant than *N. elongata* throughout the observed interval at DSDP Site 384. Both the occurrences reported by Perch-Nielsen (1976) and Bukry (1978b) are from within the *N. constricta* Zone.

Naviculopsis eobiapiculata Bukry, 1978b

1978b. *Naviculopsis eobiapiculata* n. sp.; Bukry, p. 787, pl. 4, figs 9–14.

REMARKS: Basal spines are of about the length of the basal ring, which is 40–45 µm long. Some specimens observed in Hole 752A have an apex spine. The FO *N. eobiapiculata* in Hole 752A is ~48 m (~2.6 Ma) higher than the FO *N. constricta*, which is appreciably different than the ~19 m (~1.1 Ma) between FOs of these two species recorded by Ciesielski (1991) in Hole 700B. This could be caused by contrasting species concepts in Ciesielski (1991) and this paper, but also due to palaeobiogeographic reasons.

Naviculopsis minor (Schulz) Frenguelli, 1940
(Pl. 1, Fig. 10)

1928. *Dictyocha navicula* var. *minor* n. var.; Schulz, p. 246, fig. 22.

1940. *Naviculopsis minor* (Schulz) n. comb.; Frenguelli, p. 61, fig. 11i.

REMARKS: Illustrations by Schulz (1928) and Frenguelli (1940) listed above are based on material from Kusnetzki in Russia. Other illustrated reports, by Perch-Nielsen (1976; Fur in Denmark), Martini (1981; northern Germany) and Barron *et al.* (1984; California), are all from onshore sections and thus likely from coastal waters. These illustrations show considerable variation in the basal ring size, spines lengths and arch curvature, but all display a characteristic, almost rectangular-shaped basal ring.

Naviculopsis minor is rarely recorded from deep ocean sediments. Bukry (1976) considered this taxon conspecific with *N. constricta*, but our observations show co-occurring *N. constricta* to have a decidedly smaller basal ring and longer spines. Bukry (1984) did identify *N. minor* in the late early Eocene (nannofossil zone NP13) in a short interval from Hole 553A (Rockall Plateau). The skeletal morphology is consistently present between 133.51 and 123.10 mbsf in Hole 752A (~54.0 to ~53.83 Ma; Table 5).

Naviculopsis primitiva Ciesielski, 1991
(Pl. 3, Figs 10–12; Pl. 4, Figs 1, 2)

1991. *Naviculopsis primitiva* n. sp.; Ciesielski, p. 83, pl. 9, figs 6–9.

REMARKS: This is the geologically earliest known species of *Naviculopsis*. The apical structure consists of three struts generally similar to *Corbisema*. Two of the struts attach to opposite portions of a two-sided basal ring. The third strut attaches to the general vicinity of a basal corner, with the precise location on or near the triple junction. Where the major-axis attachment is separated from the corner, the other two strut attachments may be slightly rotated in the same direction. Both dextral or sinistral rotations, seen from apical view, occur. Similar range of variation in the locations of the strut attachments is also observed on some specimens of *C. hastata alta*, and suggest a close evolutionary relationship.

In Holes 700B and 752A, the interval immediately above the *N. primitiva* Subzone contains a generally similar skeletal morphology, known as *N. cruciata*. This morphology has a fourth strut that goes to the opposite corner. Strut attachments are usually slightly rotated with respect to the major and minor axis.

Genus *Pseudonaviculopsis* McCartney, Witkowski and Szaruga gen. nov.

DESCRIPTION: Basal ring has large size and near circular to ovoid shape, often inflected at the arch attachments, and may be of robust construction. Corners (on basal ring perpendicular to the arch) are usually rounded but may be slightly pointed. Major-axis basal spines may occur. The arch has a smooth curve across the minor axis. Prominent and sometimes forked pikes can occur at or near the arch attachment. However, some skeletons lack pikes. Teratoid forms can be abundant, and include a misshaped or incomplete basal ring, an arch that has struts on one side, or multiple pikes on a basal side.

REMARKS: *Pseudonaviculopsis* constitutes a group of two-sided (naviculopsid) skeletal morphologies that is the first non-three-sided silicoflagellate skeletal morphology to occur commonly after the K/Pg extinction. This group appears in the early Palaeocene but becomes abundant near the early/middle Palaeocene boundary (~61.1 Ma) and is likely closely related to the large-sized and sometimes massively constructed *Corbisema inermis*. There is, from the early inception of the group, a range of morphologies from massively constructed to more gracile forms. The massive morphologies are more abundant in the early record, and gracile forms become more abundant and diversified with time. The early morphologies show considerable variation, especially in

the structure and placement of the pikes, and teratoid morphologies are particularly abundant.

Two of the taxa here placed within *Pseudonaviculopsis* were originally included by Ling (1981) in *Crassicorbisema* as *C. disymmetrica dumitricae* and *C. disymmetrica disymmetrica*. We accept Ling's (1981) division of the two-sided skeletons into four species and use his species nomenclature. However, we do not accept Ling's (1981) conclusion that the three-sided and two-sided forms with massive construction, which he called *C. disymmetrica dumitricae* and *C. disymmetrica disymmetrica* respectively, represent a genus distinct from the gracile two-sided morphologies of similar general shape and size. Furthermore, we believe *Crassicorbisema* was not validly published, as the description in Ling (1981) lacks a clear designation of the generitype. Even though Ling (1981) did specify "*Crassicorbisema disymmetrica* (Dumitrica) Ling comb. nov." as the type species of *Crassicorbisema*, the formal transference consists only of formal descriptions of two subspecies, both new combinations based on Dumitrică's (1973) taxonomic treatments, and no basionym is indicated for "*Crassicorbisema disymmetrica* (Dumitrica) Ling comb. nov." (Ling 1981). Two-sided skeletons are here interpreted to represent an evolutionary lineage separate from three-sided morphologies, and are thus placed into the new genus *Pseudonaviculopsis*.

OCCURRENCE: The genus is observed in Holes 208, 327A, 700B, 752A and 1121B, with a known range from the early Palaeocene to early Eocene. Gracile members of the genus have been observed in western Siberia and Denmark (Locker and Martini 1987).

GENERITYPE: *Pseudonaviculopsis disymmetrica* (Dumitrică) McCartney, Witkowski and Szaruga n. comb., n. stat.

Pseudonaviculopsis disymmetrica (Dumitrică)
McCartney, Witkowski and Szaruga comb. nov.,
stat. nov.

1973. *Corbisema inermis disymmetrica* n. subsp.; Dumitrică, p. 846, pl. 12, figs 1–6; pl. 13, figs 1–8.

1976. *Corbisema disymmetrica disymmetrica* (Dumitrică) n. comb.; Bukry, p. 891, pl. 1, figs 10–12.

1981. *Crassicorbisema disymmetrica disymmetrica* (Dumitrică) n. comb.; Ling, p. 5, pl. 1, figs 8–12.

REMARKS: This is an extremely unusual silico-

flagellate. The general range of size (usually 80–130 µm across the long axis) is consistent with the co-occurring *Pseudonaviculopsis constricta*, and we consider these two taxa to be closely related. *Pseudonaviculopsis disymmetrica* is distinguished by having remarkably thick basal elements with a reticulate ornamentation that commonly gives the basal ring a darker colour when viewed in LM. Skeletons of *Ps. disymmetrica* usually have a rounder basal ring compared to *Ps. constricta*, which tend to have a slightly more 8-shaped design. *Pseudonaviculopsis disymmetrica* also have significantly more massive and variable pikes, which can be forked, and the skeletons are more prone to be teratoid.

Dumitrica (2014) has illustrated, as a drawing, a doublet that shows paired skeletons in the Star-of-David configuration. This is consistent with the two known double skeletons of large three-sided silicoflagellates (McCartney *et al.* 2015a, figs 1b, 7d), which we believe to be ancestral to *Pseudonaviculopsis*. *Pseudonaviculopsis disymmetrica* appears to have a close phylogenetic relationship to *C. inermis crenulata*, as both have similar massive structures and surface ornamentation.

Pseudonaviculopsis constricta form *constricta*
(Busen and Wise) McCartney, Witkowski and
Szaruga comb. nov.

1976. *Corbisema navicula constricta* n. subsp.; Busen and Wise, p. 712, pl. 2, figs 7–9.

1981. *Corbisema constricta* (Busen and Wise) n. comb.; Ling, p. 4, pl. 1, figs 5–7.

REMARKS: The skeletons have basal sides indented at strut attachments, usually with small pikes. However, pikes can be absent on one or both sides. The skeletons measure up to 150 µm and have rounded corners. Skeletons that have somewhat pointed corners are placed in *Ps. cuspis*. There is considerable variability in the construction of the basal ring, with specimens that have especially robust basal elements placed in *Ps. disymmetrica*. The shapes and sizes of many skeletons of *Ps. constricta* and *Ps. disymmetrica* are similar, suggesting a close relationship, although *Ps. constricta* has a larger range of variation in both shape and size.

Pseudonaviculopsis constricta form *spinosa*
(Ciesielski) McCartney, Witkowski and Szaruga
comb. nov.

1991. *Corbisema constricta spinosa* n. sp.; Ciesielski, p. 74, pl. 1, fig. 8; pl. 3, figs 7, 8, 11, 12.

REMARKS: This taxon was not observed in the present study.

Pseudonaviculopsis cuspis (Busen and Wise)
McCartney, Witkowski and Szaruga comb. nov.

1976. *Corbisema cuspis* n. subsp.; Busen and Wise, p. 711, pl. 1, figs 4–6.

REMARKS: The basal ring is slightly pointed along the long axis. See Ling (1981) for further discussion on this taxon.

Pseudonaviculopsis naviculoidea (Frenguelli)
McCartney, Witkowski and Szaruga comb. nov.

1940. *Corbisema apiculata* f. *naviculoidea* n. form.; Frenguelli, fig. 12i.

1976. *Corbisema naviculoidea* (Frenguelli) n. comb.; Perch-Nielsen, p. 33, figs 7, 19, 22.

REMARKS: Basal sides not indented at strut attachment. Most specimens of this taxon are smaller (~50–65 µm) than the co-occurring *Ps. constricta* and are more likely to possess short basal (corner) spines along the long axis.

Genus *Stephanocha* McCartney and Jordan in Jordan and McCartney, 2015

Stephanocha? acanthica (Bukry) McCartney and Jordan in Jordan and McCartney, 2015

1978a. *Distephanus? acanthicus* n. sp.; Bukry, pp. 816, 817, fig. 6; pl. 3, figs 1–3.

part 1987. *Distephanus speculum* (Ehrenberg); Locker and Martini, pp. 46–48, pl. 5, figs 40–43.

2015. *Stephanocha? acanthica* (Bukry) n. comb.; McCartney and Jordan in Jordan and McCartney, p. 179.

REMARKS: Bukry (1978a) described this taxon based on a single essentially complete specimen that had nine basal sides and a dictyochid apical structure. We have observed rare specimens of a group of morphologies that have basal rings of similar size and shape to the specimen illustrated by Bukry (1978a). The interval between 142.5 and 123.1 mbsf in Hole 752A was

examined at higher stratigraphic resolution in order to better constrain the occurrence of this species.

Of the nine counted (Table 5) and six additional specimens of this group observed in Hole 752A, all but two have a basal ring with multiple windows and are placed in *Stephanocha? fulbrightii* sp. nov. below. The two stratigraphically highest specimens, however, have a dictyochid apical structure and are generally similar enough to Bukry's (1978a) specimens to be included in *Stephanocha? acanthica*. The specimen observed at 123.1 mbsf has seven basal sides, while that at 124.6 mbsf has six sides. Both possess a pseudofibulid apex.

Stephanocha? fulbrightii McCartney, Witkowski and Szaruga sp. nov.
(Pl. 2, Figs 4–6)

part 1987. *Distephanus speculum* (Ehrenberg); Locker and Martini, pp. 46–48, pl. 5, figs 44–49; pl. 7, figs 59, 60.

2016. *Stephanocha* sp.; McCartney and Witkowski, fig. 3-1.

DESCRIPTION: Basal ring has polygonal shape with sides that are nearly linear, slightly indented at the strut attachments, which are located at the middle of each side. There are no pikes. Basal spines are linear and usually about one-third to half the basal ring diameter long. Apical elements are of about equal lengths and form a nearly hemispherical structure made up of portals and windows of similar sizes. Apical window elements are of essentially equal lengths and usually form five-sided windows, although the apex window may have six sides. Number of basal sides and windows varies considerably.

DIFFERENTIATION: Perch-Nielsen (1976) has described two late Eocene species from the VEMA 28/43 core (Vøring Plateau, Norwegian Sea) that have an apical ring and may include multiple windows. *Stephanocha rosae* (Perch-Nielsen) McCartney and Jordan, 2015 has, in comparison to *S.? fulbrightii*, basal sides more indented at the strut attachments, struts significantly longer than the basal ring elements and a flatter apical structure. The struts attach near the middle of each side but slightly offset from small pikes. *Stephanocha norwegiensis* (Perch-Nielsen) McCartney and Jordan, 2015 has a basal ring with four or five sides, also strongly indented at the strut attachments sinistrally offset from prominent pikes. *Stephanocha? fulbrightii* differs from both of

these species in the lack of pikes and apical elements of similar size. There is also a significant difference in geologic age.

REMARKS: This is an extraordinarily unusual silicoflagellate skeletal morphology for the early Eocene. The specimens observed in Hole 752A have eight or more basal sides, but precursor silicoflagellate species that commonly have more than four basal sides are not known. Thus, the evolutionary origin of this species is problematic. McCartney and Witkowski (2016, fig. 3-1) have illustrated a skeleton from Kamyshlov, Russia, also of early Eocene age, that has five basal sides and three windows that could be conspecific with *S. fulbrightii*, or represent a closely related species. *Stephanocha? acanthica* is believed to be closely related, but the stratigraphically lower occurrence of the apically more complicated structure of *S. fulbrightii* is unexpected.

Specimens were rare, with 14 specimens observed in more than thirty microscope slides. Eight- and nine-sided forms predominate, but ten- and eleven-sided skeletons occur. The number of windows varies from two to thirteen or more, without any number predominating. One specimen with a single window was observed. Size of the basal ring is usually 40–50 µm.

We retain the question mark after the genus name previously applied by Bukry (1978a) in his description of the closely related *Stephanocha? acanthica* (see above) as we are uncertain whether this species belongs in the same evolutionary lineage as the genus that includes *Stephanocha speculum* (Stöhr) McCartney and Jordan, 2015.

OCCURRENCE: From 142.50 to 126.23 mbsf in Hole 752A, Eastern Indian Ocean, early Eocene age (~54.17 to 53.87 Ma). Five- to eight-sided specimens of roughly similar age that may be included in this species are known from Kamyshlov, Russia.

HOLOTYPE (Pl. 2, Fig. 6): SZCZ #24260 slide X (note, this is the same slide that includes the type specimen for *D. castellum*), Sample 121-752A-14X-4, 49–50 cm. Size is 40 µm between opposite basal corners.

REPOSITORY: Institute of Marine Sciences, University Szczecin Diatom Collection, Szczecin, Poland (SZCZ).

NAME DERIVATION: This species is named after United States Senator J. William Fulbright (1905–1995), who created the Fulbright Program for international exchange of scholars, in 1946.

Acknowledgements

We are grateful to Appy Sluijs, who provided sixteen Hole 752A samples (SZCZ #18014 to 18029) that initiated this study. Additional samples from Holes 752A as well as 208, 700B and 1121B were provided by the International Ocean Discovery Program. Assistance for the SEM photography of specimens was provided by Krzysztof Owocik at the Institute of Palaeobiology, Polish Academy of Sciences, Warsaw, Izabela Zgłobicka and Krzysztof J. Kurzydłowski at the Technical University of Warsaw, and Rafał J. Wróbel of the Institute of Chemical and Environment Engineering, West Pomeranian University of Technology in Szczecin. Sabine Matting translated German texts that assisted in clarifying taxonomic questions. We also thank reviewers Elisa Malinverno and Sherwood W. Wise, Jr., editor Anna Zylińska, Richard Jordan and David Harwood for useful comments. A research sabbatical from the University of Maine at Presque Isle and a scholarship from the Polish-American Fulbright Commission provided the first author with opportunity to do this research in Szczecin, Poland. Parts of this research were supported by the Polish National Science Centre grant no. 2014/13/B/ST10/02988.

REFERENCES

- Barron, J.A., Bukry, D. and Poore, R.Z. 1984. Correlation of the middle Eocene Kellogg Shale of northern California. *Micropaleontology*, **30**, 138–170.
- Barron, J.A., Stickley, C.E. and Bukry, D. 2015. Paleoceanographic, and paleoclimatic constraints on the global Eocene diatom and silicoflagellate record. *Palaeogeography, Palaeoclimatology, Palaeoecology*, **422**, 85–100.
- Bukry, D. 1973. Coccolith and silicoflagellate stratigraphy, Tasman Sea and Southwestern Pacific Ocean, Deep Sea Drilling Project Leg 21. In: Burns, R.E., Andrews, J.E. *et al.* (Eds), *Initial Reports of the Deep Sea Drilling Project, Scientific Results*, **21**, 885–893.
- Bukry, D. 1975. Silicoflagellate and coccolith stratigraphy, Deep Sea Drilling Project Leg 29. In: Kennett, J.P., Houtz, R.E. *et al.* (Eds), *Initial Reports of the Deep Sea Drilling Project, Scientific Results*, **29**, 845–872.
- Bukry, D. 1976. Cenozoic silicoflagellate and coccolith stratigraphy, South Atlantic Ocean, Deep Sea Drilling Project Leg 36. In: Hollister, C.D., Craddock, C. *et al.* (Eds), *Initial Reports of the Deep Sea Drilling Project, Scientific Results*, **35**, 885–917.
- Bukry, D. 1977a. Coccolith and silicoflagellate stratigraphy, Central North Atlantic Ocean, Deep Sea Drilling Project Leg 37. In: Aumento, F., Perch-Nielsen, K. *et al.* (Eds), *Initial Reports of the Deep Sea Drilling Project, Scientific Results*, **39**, 825–839.
- Bukry, D. 1977b. Coccolith and silicoflagellate stratigraphy,

- South Atlantic Ocean, Deep Sea Drilling Project Leg 39. In: Supko, P.R., Melson, W.G. *et al.* (Eds), *Initial Reports of the Deep Sea Drilling Project, Scientific Results*, **37**, 917–927.
- Bukry, D. 1978a. Cenozoic coccolith, silicoflagellate, and diatom stratigraphy, Deep Sea Drilling Project Leg 44. In: Benson, W.E., Sheridan, R.E. *et al.* (Eds), *Initial Reports of the Deep Sea Drilling Project, Scientific Results*, **50**, 507–523.
- Bukry, D. 1978b. Cenozoic silicoflagellate and coccolith stratigraphy, northwestern Atlantic Ocean, Deep Sea Drilling Project Leg 43. In: Benson, W.E., Sheridan, R.E. *et al.* (Eds), *Initial Reports of the Deep Sea Drilling Project, Scientific Results*, **44**, 775–805.
- Bukry, D. 1978c. Cenozoic silicoflagellate and coccolith stratigraphy, southeastern Atlantic Ocean, Deep Sea Drilling Project Leg 40. In: Bolli, H.M., Ryan, W.B.F. *et al.* (Eds), *Initial Reports of the Deep Sea Drilling Project, Scientific Results*, **40**, 635–649.
- Bukry, D. 1981. Synthesis of silicoflagellate stratigraphy for Maastrichtian to Quaternary marine sediment. *SEPM Special Publication*, **32**, 433–444.
- Bukry, D. 1982. Cenozoic silicoflagellates from offshore Guatemala, Deep Sea Drilling Project Site 495. In: Aubouin, J., von Huene, R. *et al.* (Eds), *Initial Reports of the Deep Sea Drilling Project, Scientific Results*, **67**, 425–445.
- Bukry, D. 1984. Cenozoic silicoflagellates from Rockall Plateau, Deep Sea Drilling Project Leg 81. In: Roberts, D.G., Schnitker, D. *et al.* (Eds), *Initial Reports of the Deep Sea Drilling Project, Scientific Results*, **81**, 547–563.
- Bukry, D. 1987. Eocene siliceous and calcareous phytoplankton, Deep Sea Drilling Project Leg 95. In: Poag, C.W., Watts, A.B. *et al.* (Eds), *Initial Reports of the Deep Sea Drilling Project, Scientific Results*, **95**, 395–415.
- Bukry, D. and Foster, J.H. 1974. Silicoflagellate zonation of upper Cretaceous to lower Miocene deep sea sediment. *Journal Research U.S. Geological Survey*, **2**, 303–310.
- Busen, K.E. and Wise Jr., S.W. 1976. Silicoflagellate stratigraphy, Deep Sea Drilling Project, Leg 36. In: Barker, P.F., Dalziel, I.W.D. *et al.* (Eds), *Initial Reports of the Deep Sea Drilling Project, Scientific Results*, **36**, 697–743.
- Ciesielski, P.F. 1991. Biostratigraphy of diverse silicoflagellate assemblages from the Early Paleocene to Early Miocene of Holes 698A, 700B, 702B, and 703A: Subantarctic South Atlantic. In: Ciesielski, P.F., Kristoffersen, Y. *et al.* (Eds), *Proceedings of the Ocean Drilling Program, Scientific Results*, **114**, 49–96.
- Crux, J.A. 1991. Calcareous nannofossils recovered by Leg 114 in the Subantarctic South Atlantic Ocean. In: Ciesielski, P.F., Kristoffersen, Y. *et al.* (Eds), *Proceedings of the Ocean Drilling Program, Scientific Results*, **114**, 155–177.
- Deflandre, G. 1950. Contribution à l'étude des silicoflagellés actuels et fossiles. *Microscopie*, **2**, 72–108, 117–142, 191–210.
- Dumitrică, P. 1973. Paleocene, late Oligocene and post-Oligocene silicoflagellates in southwestern Pacific sediments cored on DSDP Leg 21. In: Burns, R.E., Andrews, J.E. *et al.* (Eds), *Initial Reports of the Deep Sea Drilling Project, Scientific Results*, **21**, 837–883.
- Dumitrica, P. 2014. Double skeletons of silicoflagellates: Their reciprocal position and taxonomical and paleobiological values. *Revue de Micropaléontologie*, **57**, 57–74.
- Ehrenberg, C.G. 1839. Über die Bildung der Kreidefelsen und des Kreidemergels durch unsichtbare Organismen. *Königlich Preussische Akademie der Wissenschaften zu Berlin*, **1838**, 59–148.
- Fenner, J.M. 1991. Taxonomy, stratigraphy, and paleoceanographic implications of Paleocene diatoms. In: Ciesielski, P.F., Kristoffersen, Y. *et al.* (Eds), *Proceedings of the Ocean Drilling Program, Scientific Results*, **114**, 123–154.
- Fenner, J.M. 2015. Description of a new fossil diatom species, *Haslea antiqua* (Bacillariophyceae), with comments on its valve structure, and habitat. In: J. Witkowski, D. Williams and J.P. Kocielek (Eds), *Diatoms and the continuing relevance of morphology to studies on taxonomy, systematics and biogeography*. *Nova Hedwigia, Beiheft*, **144**, 107–124.
- Fourtanier, E. 1991. Paleocene and Eocene diatom biostratigraphy and taxonomy of eastern Indian Ocean Site 752. In: J. Peirce, J. Weissel *et al.* (Eds), *Proceedings of the Ocean Drilling Program, Scientific Results*, **121**, 171–187.
- Freguelli, J. 1940. Consideraciones sobre los silicoflagelados fósiles. *Revista del Museo de la Plata, Paleontología*, **7**, 37–112.
- Glezer, Z.I. 1960. Silicoflagellates of the Paleocene. *Informatsonnyi Sbornik VSEGEI*, **35**, 127–136. [In Russian]
- Glezer, Z.I. 1964. New silicoflagellates of the Palaeogene of the USSR. *Novosti sistematiki nizshikh rastenij*, **1**, 46–58. [In Russian]
- Glezer, Z.I. 1966. Silicoflagellatophyceae. In: Gollerbakh, M.M. (Ed.), *Cryptogamic Plants of the S.S.S.R.* (Vol. 7), 363 p. V.A. Komarova Botanical Institute. [Translated from Russian by the Israel Program for Scientific Translations Ltd, Jerusalem, 1970]
- Glezer, Z.I. 1979. On Paleocene zonal stratigraphy of Mediterranean paleogeographic region in the USSR based on silicoflagellate algae. *Proceedings of the 22nd Session of the All-Russia Paleontological Society*, pp. 29–42. Nauka; Leningrad. [In Russian]
- Gombos Jr., A.M. 1984. Late Paleocene diatoms in the Cape Basin. In: Hsü, K.J., LaBrecque, J.L. *et al.* (Eds), *Initial Reports of the Deep Sea Drilling Project, Scientific Results*, **73**, 495–511.
- Gradstein, F.M., Ogg, J.G., Schmitz, M.D. and Ogg, G.M. 2012. *The Geologic Time Scale 2012*. Volume 2, 1144 p. Elsevier; Amsterdam.

- Haeckel, E.H.P.A. 1894. Systematische Phylogenie. Entwurf eines Natürlichen Systems der Organismen auf Grund ihrer Stammesgeschichte. Erster Theil: Systematische Phylogenie der Protisten und Pflanzen, 400 p. Georg Reimer; Berlin.
- Hanna, G.D. 1928. Silicoflagellata from the Cretaceous of California. *Journal of Paleontology*, **1**, 159–163, 259–263
- Hanna, G.D. 1931. Diatoms and silicoflagellates of the Kreyenhagen Shale. *Mining in California*, **27** (2), 197–201.
- Harwood, D.M. 1988. Upper Cretaceous and lower Paleocene diatom and silicoflagellate biostratigraphy of Seymour Island, Eastern Antarctic peninsula. In: Feldmann, R. and Woodburne, M.D. (Eds), *Geology and Paleontology of Seymour Island. Geological Society of America Memoir*, **169**, 55–129.
- Hay, W.W., DeConto, R.M., Wold, C.N., Wilson, K.M., Voigt, S., Schulz, M., Wold, A.R., Dullo, W.-C., Ronov, A.B., Balukhovskiy, A.N. and Söding, E. 1999. Alternative global Cretaceous paleogeography. *Geological Society of America Special Paper*, **332**, 1–47.
- Hollis, C.J. 2002. Biostratigraphy and paleoceanographic significant of Paleocene radiolarians from offshore eastern New Zealand. *Marine Micropaleontology*, **46**, 265–316.
- Kim, B.I. and Glezer, Z.I. 2007. Sedimentary cover of the Lomonosov Ridge: Stratigraphy, structure, deposition history, and ages of seismic facies units. *Stratigraphy and Geological Correlation*, **15** (4), 401–420.
- Jordan, R.W. and McCartney, K. 2015. *Stephanocha* nom. nov., a replacement name for the illegitimate silicoflagellate genus *Distephanus* (Dictyochophyceae). *Phytotaxa*, **201** (3), 177–187.
- Lazarus, D., Barron, J., Renaudie, J., Diver, P. and Türke, A. 2014. Cenozoic Planktonic Marine Diatom Diversity and Correlation to Climate Change. *PLoS ONE*, **9** (1), e84857. doi: 10.1371/journal.pone.0084857.
- Lemmermann, E. 1901. Silicoflagellatae. *Deutsche Botanische Gesellschaft, Berichte*, **19**, 247–271.
- Ling, H.-Y. 1981. *Crassicorbisema*, a new silicoflagellate genus, from the Southern Oceans and Paleocene silicoflagellate zonation. *Transactions and Proceedings of the Paleontological Society of Japan*, **121**, 1–13.
- Locker, S. and Martini, E. 1987. Silicoflagellaten aus einigen russischen Paläogen-Vorkommen. *Senckenbergiana lethaea*, **68**, 21–67.
- Martini, E. 1981. Silicoflagellaten im Paläogen von Norddeutschland. *Senckenbergiana lethaea*, **62**, 277–283.
- McCartney, K., Abe, K., Harrison, M.A., Witkowski, J., Harwood, D.M., Jordan, R.W. and Kano, H. 2015a. Silicoflagellate double skeletons in the geologic record. *Marine Micropaleontology*, **117**, 65–79.
- McCartney, K., Abe, K., Jordan, R.W. and Witkowski, J. 2015b. Morphological variation in pike structure in *Corbisema* (Silicoflagellata) from the Eocene. *Journal of Nannoplankton Research*, **35**, 177–184.
- McCartney, K., Abe, K., Witkowski, J. and Jordan, R.W. 2014a. Two rare silicoflagellate double skeletons of the Star-of-David configuration from the Eocene. *Journal of Micropaleontology*, **34**, 97–99.
- McCartney, K., Churchill, S. and Woestendiek, L. 1995. Silicoflagellates and ebridians from ODP Leg 138, Eastern Equatorial Pacific. In: Pisias, N.G., Mayer, L.A. et al. (Eds), *Proceedings of the Ocean Drilling Program, Scientific Results*, **138**, 129–162.
- McCartney, K. and Harwood, D.M. 1992. Silicoflagellates from Leg 120 on the Kerguelen Plateau, Southeast Indian Ocean. In: Wise, S.W. Jr., Schlich, R. et al. (Eds), *Proceedings of the Ocean Drilling Program, Scientific Results*, **120**, 811–831.
- McCartney, K., Harwood, D.M. and Witkowski, J. 2010a. A rare double skeleton of the silicoflagellate *Corbisema*. *Journal of Micropaleontology*, **29**, 185–186.
- McCartney, K., Harwood, D.M. and Witkowski, J. 2011a. Late Cretaceous silicoflagellate taxonomy and biostratigraphy of the Arctic Margin, Northwest Territories, Canada. *Micropaleontology*, **57**, 61–86.
- McCartney, K. and Wise, Jr., S.W. 1987. Silicoflagellates and ebridians from Deep Sea Drilling Project Leg 93, Site 604 and 605 (New Jersey Transect). In: van Hinte, J.E., Wise, S.W. Jr. et al. (Eds), *Initial Reports of the Deep Sea Drilling Project, Scientific Results*, **93**, 801–814.
- McCartney, K. and Witkowski, J. 2016. Cenozoic silicoflagellate skeletal morphology: A review and suggested terminology. *Journal of Micropaleontology*, **35**, 179–189.
- McCartney, K., Witkowski, J. and Harwood, D.M. 2010b. Early Evolution of the Silicoflagellates during the Cretaceous. *Marine Micropaleontology*, **77**, 83–100.
- McCartney, K., Witkowski, J. and Harwood, D.M. 2011b. Unusual early assemblages of Late Cretaceous silicoflagellates from the Canadian Archipelago. *Revue de Micropaleontologie*, **54**, 31–58.
- McCartney, K., Witkowski, J., Jordan, R.W., Daughjerg, N., Malinverno, E., van Wezel, R., Kano, H., Abe, K., Scott, F., Schweizer, M., Young, J.R., Hallegraef, G.M. and Shiozawa, A. 2014b. Fine structure of silicoflagellate double skeletons. *Marine Micropaleontology*, **113**, 10–19.
- Perch-Nielsen, K. 1975. Late Cretaceous to Pleistocene silicoflagellates from the southern southwest Pacific, DSDP, Leg 29. In: Kennett, J.P., Houtz, R.E. et al. (Eds), *Initial Reports of the Deep Sea Drilling Project, Scientific Results*, **29**, 677–721.
- Perch-Nielsen, K. 1976. New silicoflagellates and a silicoflagellate zonation in north European Palaeocene and Eocene diatomites. *Bulletin of the Geological Society of Denmark*, **25**, 27–40.
- Percival Jr., S.F. 1984. Late Cretaceous to Pleistocene calcareous nannofossils from the South Pacific, Deep Sea Drilling Project Leg 73. In: Hsü, K.J., LaBrecque, J.L. et al. (Eds),

- Initial Reports of the Deep Sea Drilling Project, Scientific Results*, **73**, 391–424.
- Pospichal, J.J., Dehn, J., Driscoll, N.W., and fourteen others 1991. Cretaceous–Paleogene biomagnetostratigraphy of Sites 752–755, Broken Ridge: A synthesis. In: Peirce, J., Weissel, J. et al. (Eds), *Proceedings of the Ocean Drilling Program, Scientific Results*, **121**, 721–741.
- Schulz, P. 1928. Beiträge zur Kenntnis fossiler und rezenter Silicoflagellaten. *Botanischen Archiv*, **21**, 225–292.
- Shaw, C.A. and Ciesielski, P.F. 1983. Silicoflagellate biostratigraphy of middle Eocene to Holocene subantarctic sediments recovered by Deep Sea Drilling Project Leg 71. In: Ludwig, W.J., Krashennnikov, V.A. et al. (Eds), *Initial Reports of the Deep Sea Drilling Project, Scientific Results*, **71**, 687–737.
- Silva, P.C. 1980. Names of classes and families of living algae. *Regnum Vegetabile*, **103**, 1–156.
- Tsoy, I.B. 2011. Silicoflagellates of the Cenozoic of the Japan and Okhotsk Seas and the Kuril-Kamchatka Trench, 224 p. Russian Academy of Sciences; Vladivostok. [In Russian]
- Tsutsui, H., Jordan, R.W., Nishiwaki, N. and Nishida, S. 2018. Morphometric analysis of early Eocene *Corbisema* skeletons (Silicoflagellata) in Mors, Denmark. *Journal of Micropalaeontology*, **37**, 283–293.
- Whitehead, J. and Bohaty, S.M. 2003. Pliocene summer sea surface temperature reconstruction using silicoflagellates from Southern Ocean ODP Site 1165. *Paleoceanography*, **18** (3), 1075. doi: 10.1029/2002PA000829.
- Witkowski, J., Bohaty, S.M., McCartney, K. and Harwood, D.M. 2012. Enhanced siliceous plankton productivity in response to middle Eocene warming at Southern Ocean ODP Sites 748 and 749. *Palaeogeography, Palaeoclimatology, Palaeoecology*, **326–328**, 78–94.
- Zittel, K.A. 1876. Uebereinige fossile radiolarien aus der norddeutschen Kreide. *Zienschaft der deutschen geologischen Gesellschaft*, **18**, 75–86.

Manuscript submitted: 30th August 2017

Revised version accepted: 16th January 2018

PLATES 1–4

PLATE 1

LM micrographs of silicoflagellates from DSDP Legs 21 (Figs 1, 2), 73 (Fig. 9), ODP Legs 114 (Figs 4, 8), 121 (Figs 3, 5–7, 10)

1, 5 – *Corbisema* cf. *trigona* (Zittel) Hanna, 1928; **1** – apical view, sample 208-30R-3, 50–51 cm; **5** – apical view, sample 208-30R-4, 50–51 cm; **2, 3** – *Corbisema* aff. *archangelskiana* (Schulz) Frenguelli, 1940; **2** – abapical view, sample 752A-14X-3, 63–64 cm; **3** – slightly disarticulated double skeleton, apical axis view, sample 752A-14X-4, 49–50 cm; **4** – *Corbisema archangelskiana* (Schulz) Frenguelli, 1940; four-sided variant, apical view, sample 114-700B-30-3, 105–106 cm; **6** – *Naviculopsis* cf. *americana* Bukry in Barron *et al.*, 1984; apical view, 752A-15X-4, 62–64 cm; **7** – *Dictyocha prearentis* Bukry, 1976; abapical view, sample 752A-15X-4, 62–64 cm; **8** – *Corbisema cunicula* (Bukry) McCartney, Witkowski and Szaruga n. comb. et n. stat.; abapical view, sample 700B-30-1, 79–80 cm; **9** – *Naviculopsis danica* Perch-Nielsen, 1976; abapical view, 524-4R-3, 87–89 cm; **10** – *Naviculopsis minor* (Schulz) Frenguelli, 1940; apical view, sample 752A-14X-3, 120–121 cm.

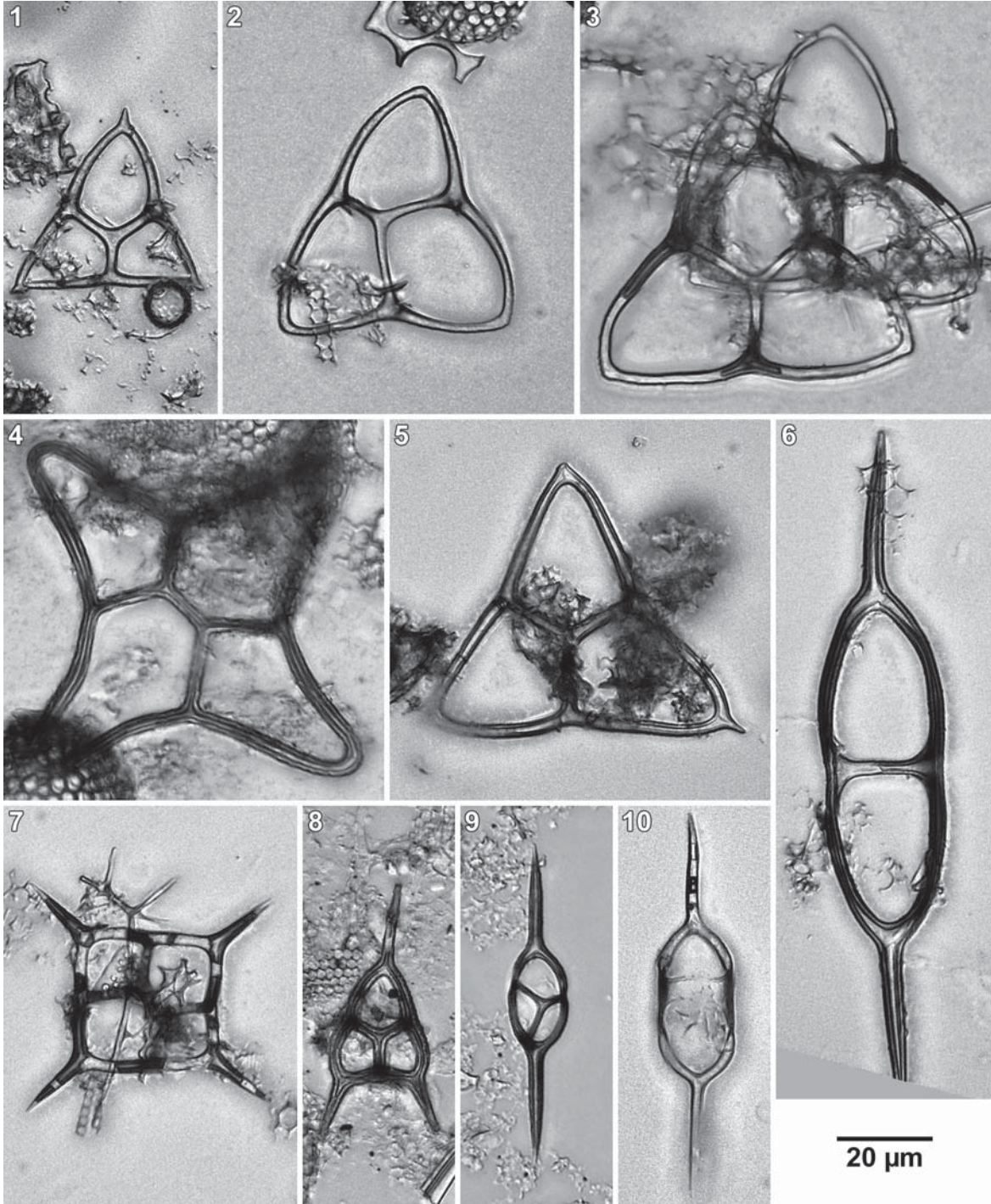


PLATE 2

LM micrographs of silicoflagellates from ODP Leg 121

1-3 – *Dictyochoa castellum* McCartney, Witkowski and Szaruga sp. nov.; 1 – abapical view, sample 752A-14X-1, 49–50 cm; 2 – apical view, holotype, sample 752A-14X-1, 49–50 cm; 3 – apical view, sample 752A-14X-5, 20–21 cm; **4-6** – *Stephanopsis? fulbrightii* McCartney, Witkowski and Szaruga sp. nov.; 4 – apical view, sample 752A-15X-4, 62–64 cm; 5 – apical view, sample 752A-14X-1, 49–50 cm; 6 – apical view, holotype, sample 752A-14X-1, 49–50 cm; **7** – *Corbisema apiculata* (Lemmermann) Hanna, 1931; double skeleton, apical axis view, sample 752A-14X-1, 49–50 cm.

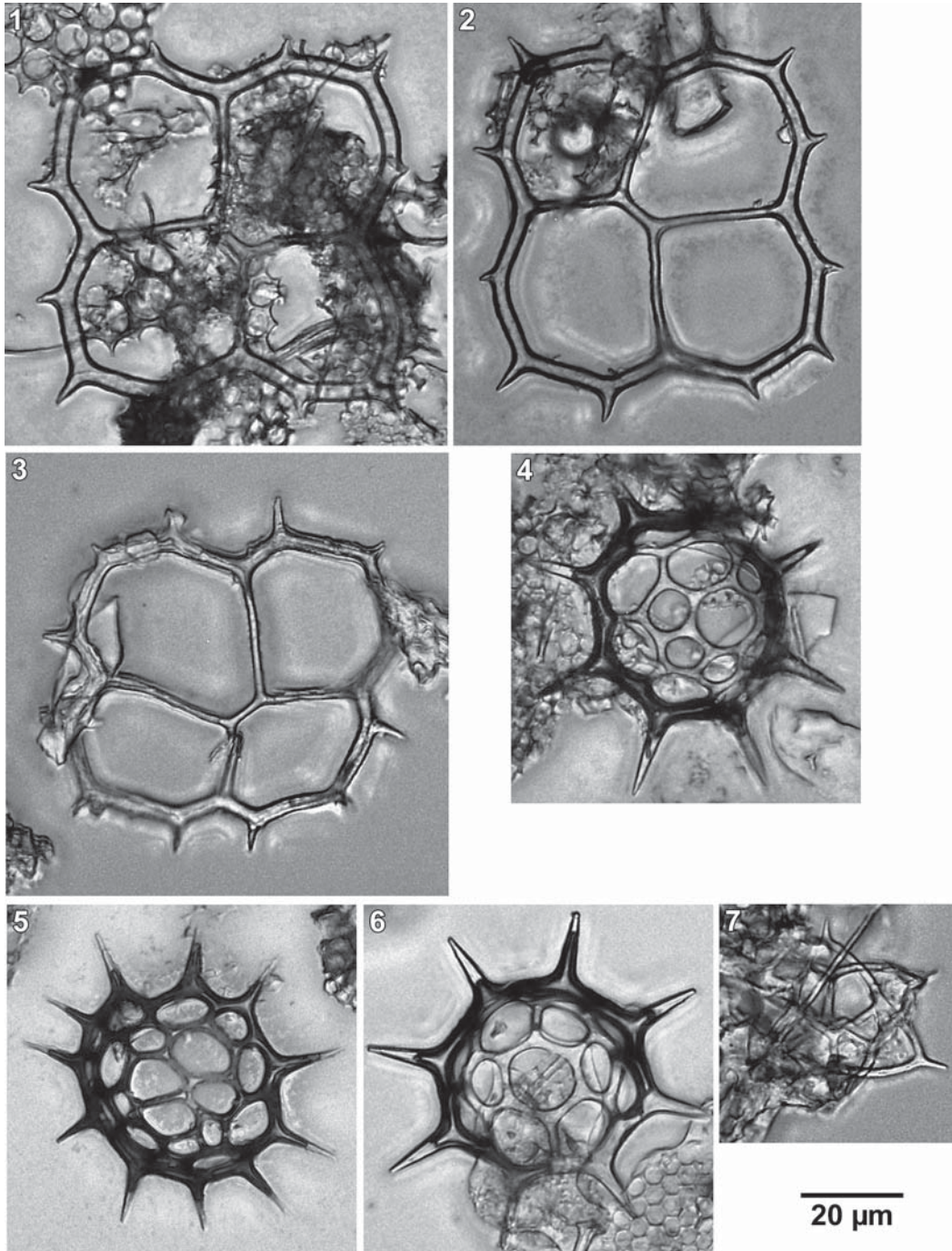


PLATE 3

LM micrographs of silicoflagellates from ODP Legs 114 (1–4, 6–9) and 121 (5, 10–12)

1-6 – *Corbisema hastata alta* Ciesielski, 1991; 1-4, 6. sample 700B-30-3, 105–106 cm; 1-3 – apical view; 4 – abapical view; 6 – lateral view; 5 – sample 752A-28-4, 120–121 cm, apical view; **7-9** – *Naviculopsis cruciata* Ciesielski, 1991; 7 – sample 700B-30-1, 135–136 cm, abapical view; 8, 9 – sample 700B-27-4, 80–81 cm, abapical view; **10-12** – *Naviculopsis primitiva* Ciesielski, 1991; 10 – sample 121-752A-28-2, 126–127 cm, lateral view; 11 – sample 121-752A-28-3, 20–21 cm, apical view; 12 – sample 121-752A-28-2, 126–127 cm, abapical view.

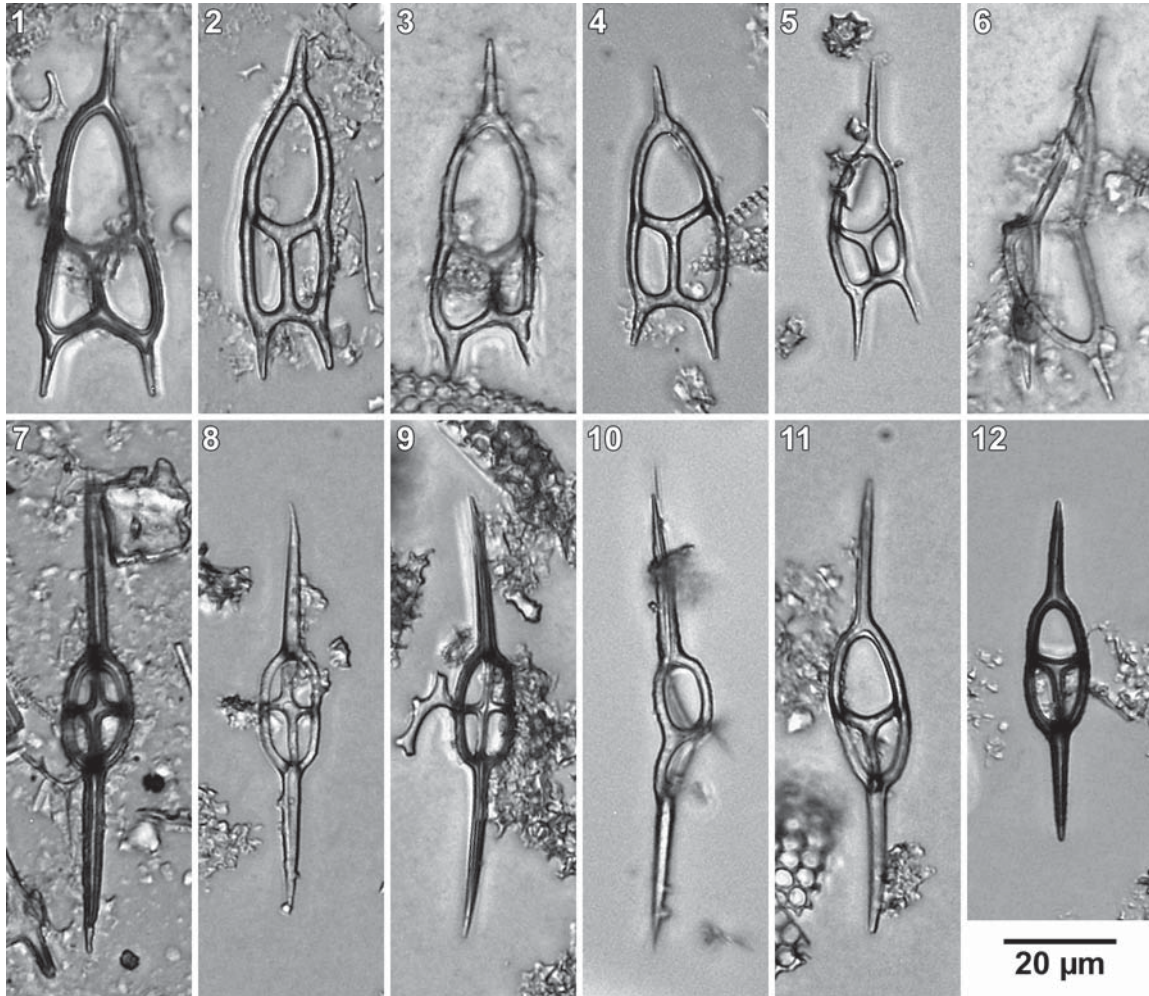


PLATE 4

SEM micrographs of silicoflagellates from ODP Legs 114 (Figs 1–3), 121 (Figs 4–7)

1, 2 – *Naviculopsis primitiva* Ciesielski, 1991; sample 700B-30R-1, 135–136 cm; 1 – lateral view; 2 – apical view; **3** – *Naviculopsis cruciata* Ciesielski, 1991; apical view, sample 700B-30R-1, 121–122 cm; **4, 5** – *Naviculopsis* cf. *americana* Bukry in Barron *et al.*, 1984; apical view, 752A-15X-4, 62–64 cm; 4 – apical view; 5 – abapical view; **6** – *Corbisema apiculata* (Lemmermann) Hanna, 1931; apical view, 752A-15X-4, 62–64 cm; **7** – *Corbisema* cf. *byronalis* Bukry in Barron *et al.*, 1984; apical view, 752A-15X-4, 62–64 cm.

